2013

Development of a smart timber bridge--sensor evaluation and data processing techniques

Trevor Pence
Iowa State University

Development of a smart timber bridge—sensor evaluation and data processing techniques

by

Trevor Lee Pence

A thesis submitted to the graduate faculty

in partial fulfillment of requirements for the degree of

MASTER OF SCIENCE

Major: Civil Engineering (Structural Engineering)

Program of Study Committee:
Brent M. Phares, Co-Major Professor
Terry J. Wipf, Co-Major Professor
Douglas Stokke

Iowa State University

Ames, Iowa

2013

TABLE OF CONTENTS

LIST OF FIGURES

LIST OF TABLES

ABSTRACT

The critical deterioration of bridges nationwide has initiated the search for new methods to rehabilitate, repair, manage, and construct bridges. Consequently, smart structure concepts utilizing structural health monitoring strategies have emerged to help improve future bridge management. However, in the specific case of timber bridges, a limited amount of research has been conducted on long-term structural health monitoring solutions. To date, timber bridge evaluation efforts have focus primarily on visual inspection data to determine the structural integrity of timber structures. To improve current timber bridge inspection and management strategies, a five-year research plan to develop a smart timber bridge structure was undertaken. The overall goal is to develop a turn-key system to analyze, monitor, and report on the performance and condition of timber bridges.

This paper outlines two of the multiple phases in the five-year research plan. One phase focusses on developing, embedding, and attaching both strain and moisture sensors into glued-laminated (glulam) timber components. The other phase addresses data processing techniques to determine structural stiffness changes in timber bridges.

From this work, the following contributions were added to the development of the smart timber bridge.

- A commercially available timber moisture sensor was selected for the smart timber bridge due its reasonable accuracy, survivability under repeated loading, and ability to be wired in to a complete data logging system.
- Two methods for embedding and attaching strain sensors into glulam girders were developed, tested, and successfully integrated into the glulam fabrication process.
- A data processing technique to evaluate structural stiffness parameters was successfully developed and implemented on an existing timber bridge.

The timber specific sensors and data processing techniques described herein collectively advance the development of the smart timber bridge. Upon completing the ongoing research plan, timber bridge owners will be provided with useful information regarding the performance and condition of their structure. As a result, owners will be able to program routine maintenance and/or rehabilitation in a more timely fashion.

CHAPTER 1 GENERAL INTRODUCTION

1.1 Background

Recently, much attention has been given toward the development of an intelligent infrastructure. The idea is to develop and deploy civil systems that have sensors integrated into them such that the condition and performance of the system can be reported on continuously and, generally, remotely. In the case of timber bridges, traditional condition assessments have been determined by visual inspection and basic testing of the structure's members with maintenance decisions being based upon gathered information. To improve this situation, a conceptual smart timber bridge was developed with the purpose of improving the long-term performance, maintenance, and management of timber bridges.

Several recent technological advances have resulted in the development of cost effective sensing and communications systems. Although not yet turnkey systems, the potential exists to develop timber bridges that, using quantitative sensed information, report on their performance and condition.

1.2 Objective and Scope

The objective of this work is to continue the development of a smart timber bridge with a specific interest in timber sensing capabilities and data processing techniques. The developed sensors and data processing methods presented herein have the potential to be integrated into a smart timber bridge capable of monitoring and reporting the condition over the long-term.

1.3 Thesis Organization

The remainder of Chapter 1 presents a literature review of previous research conducted on timber moisture sensing. Chapters 2 and 3 correspond to the research goals presented above. Specifically, Chapter 2 presents a journal paper prepared for submission to the *Transportation Research Record: Journal of the Transportation Research Board*. The paper discusses the selection, implementation, and evaluation of various moisture and strain sensors specific to timber structures. Chapter 3 also presents a journal paper submitted to the *Transportation Research Record: Journal of the Transportation Research Board*. This paper focusses on data processing techniques to assess changes in timber bridge structural stiffness. Both projects are a cooperative effort between the USDA Forest Service, Forest Products

Laboratory (FPL) and the Iowa State University Bridge Engineering Center (BEC). Note Chapters 2 and 3 provide addition background information and a brief literature review.

Finally, Chapter 4 summarizes the conclusions drawn from the two papers and plans for future work in the development of a smart timber bridge. References for each chapter's contents are given at the end of the individual chapters.

1.4 Literature Review

This section presents a synopsis of previous research concerning the use of moisture sensors in civil engineering structures. Traditional methods of detecting moisture in wood will be discussed along with advanced methods currently in use. Although timber structures are the main focus of this research, an overview of concrete moisture sensors will be provided for completeness.

1.4.1 Traditional Methods for Determining Moisture Content in Timber Structures

The moisture content of wood (MC) is defined as the weight of water in wood given as a percentage of oven dry weight (Wood Handbook, 1999). The purpose of measuring moisture is to determine areas with potential decay activity.

As wood decays, the electrical properties of the material are altered. Electrical resistance type moisture meters are the most common and simplest tool to measure the moisture content in wood. Moisture meters measure the electrical resistance between two pins driven into the wood and relate the resistance to a moisture content as shown in Figure 1 (Wood Handbook, 1999). The variation shown by the shaded region in Figure 1 is generally due to differences between wood species. For a given resistance, the moisture content can vary as much as 10% if the species is unknown. Many commercially available moisture meters apply species and temperature correction factors to achieve more accurate moisture content readings. ASTM D4444-08 outlines the procedure for using moisture meters to determine the moisture content in wood (ASTM D4444, 2008). Moisture meters have been proven to be an effective tool for timber bridge inspections. Although great for inspection purposes, moisture meters cannot be used to monitor the moisture content remotely and continuously over time; the goal of structural health monitoring.

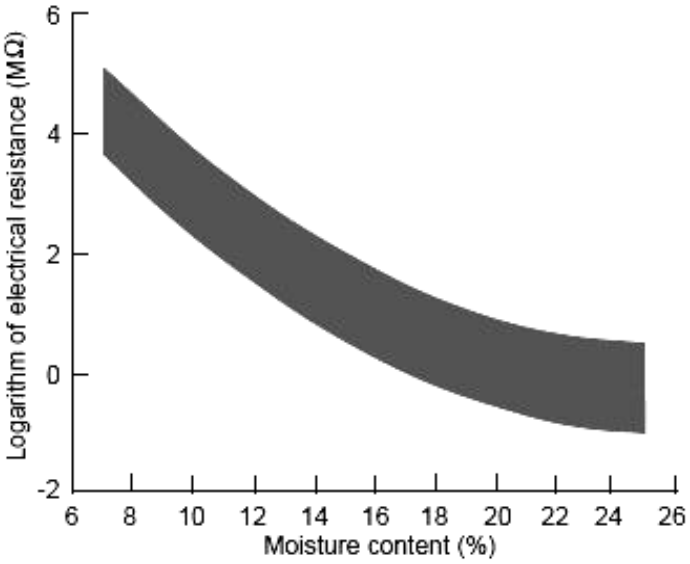

Figure 1: Relationship Between Electrical Resistance in Wood and Moisture Content.

Other ASTM standards are available to measure moisture content in wood. *Standard Test Methods for Direct Moisture Content Measurement of Wood and Wood-Base Materials* outlines four test methods to measure moisture content (ASTM D4442, 2007). Method A is intended as the sole primary method and is used when high levels of accuracy are needed (e.g., research). Method A, the oven-dry method, requires pulverizing the wood material to saw dust. Then, the original mass of the sawdust is determined and compared to the oven dry mass to determine the moisture content. Method B is also an oven dry method; however, the method differs from method A in that the specimen can be a solid piece of wood instead of sawdust. Method C, the distillation method, is intended for materials that have been chemically treated where oven-drying procedures induce greater error. The method uses an extraction apparatus and chemicals to measure the amount of water extracted from the specimen. The final method, Method D, accepts other methods to determine moisture content as long as the general practices and intent of the oven-dry and other methods are employed. Other methods include: Karl Fischer titration, infrared (heating and absorption), microwave, nuclear magnetic resonance (NMR), vacuum-oven drying, etc. The above methods are for laboratory experiments; therefore, the methods are not feasible for the in situ measurements required for this work.

1.4.2 Monitoring the Moisture Content of Timber Bridges (Dyken and Kepp, 2010)

Treteknisk (Norwegian Institute for Wood Technology) has instrumented five Norwegian timber bridges to monitor the moisture content over time. They instrumented the bridges by embedding relative humidity/temperature sensors into various timber members. The moisture content of timber depends on both the relative humidity and temperature of the air surrounding it. Therefore, by embedding a relative humidity/ temperature sensor in a small void within the wood, an equilibrium moisture content (EMC) can be obtained assuming the moisture content of the wood is in equilibrium with the humidity of the air. The relationship between relative humidity, temperature, and EMC is shown in Equation 1.

$$EMC = \frac{(1{,}800\ Kh)}{W(1-Kh)} + \frac{K_1 Kh + 2K_1K_2K^2h^2}{1+K_1Kh+K_1K_2K^2h^2} \quad (1)$$

Where:

W = 330 + 0.452T + .00415T^2

K = 6034 + 0.000463T - .000000844T^2

K_1= 6.34 + 0.000775T - .0000935T^2

K_2 = 1.91 + 0.0407T – 0.000293T^2

T = Temperature (Fahrenheit)

h = Relative Humidity

Results from testing yielded moisture contents that varied significantly with temperature. Furthermore, the EMC values varied a substantial amount within a short period of time, which was considered improbable. However, the long term averages of moisture content seem to be reasonable. A conclusion was made that the influence of temperature is suspected to artificially skew the calculated moisture content using Equation 1. In an effort to obtain more accurate results, laboratory tests were carried out to establish a new formula.

The idea of the laboratory tests was to keep the moisture content constant, vary the temperature, and see how the relative humidity changes. Various specimens with known moisture content were embedded with Vaisala Humitters and completely sealed off with adhesive tape to keep the moisture content constant. After four series of laboratory tests, a

substantial amount of data were available. The specimens had moisture contents that ranged from 6.2% to 21.3% while the temperature ranged from 29.5 C to -30.3 C. The test results confirmed that Equation 1.1 could be used as an approximation to calculate moisture content; however, a new equation had to be developed in order to eliminate the short term temperature effects on the calculated moisture content. To establish a new formula, moisture content was plotted as a function of relative humidity at various temperatures. A quadratic polynomial best fit line was chosen to approximate the data. The new equation is shown in Equation 2.

$$\mathrm{MC}\,(\mathrm{RH},\mathrm{T}) = \left((a_A T^2 + b_A T + c_A)RH^2\right) + \left((a_B T^2 + b_B T + c_B)\,RH\right) + (a_C T^2 + b_C T + c_C) \qquad (2)$$

Where:

T = Temperature (Celsius)

RH = Relative humidity(%)

Table 1: Equation 1.2 Coefficients

	a	b	c
A	$0.57x10^{-6}$	$29.34x10^{-6}$	$1.17007x10^{-3}$
B	$70.3x10^{-6}$	$2.8933x10^{-6}$	$87.6041x10^{-3}$
C	$2.0553x10^{-3}$	$2.4551x10^{-3}$	4.181162

The new equation was applied to the five Norwegian bridges mentioned earlier. Equation 2 results in less moisture content variation over time compared to Equation 1. However, Equation 2 fluctuates slightly due to large temperature variations. In addition, the new equation indicates that the wood moisture content is slightly higher than what Equation 1 implies. However, both equations are below the ambient EMC, which implies the structure dries out over time. A conclusion was drawn that wood may not attain an EMC relating to the ambient climate. Therefore, one should never assume the moisture content of wood based on ambient conditions.

1.4.3 Monitoring the Performance of Timber Bridges over the Long Term (Wacker et al. 2007)

The Forest Products Laboratory (FPL) conducted a preliminary study to monitor the performance of timber bridges over the long term. One component of the study was to evaluate the performance of wood moisture sensors. The goal was to outline sensor types and features needed to obtain reliable data to successfully monitor moisture in timber bridges.

The approach was to subject a small scale birch beam to controlled moisture conditions (i.e., 70°F and relative humidity 12%) and evaluate the change in the wood moisture content over a 60-day period. The specimen was a 5 in. x 5 in. x 48 in. birch beam equipped with two different types of moisture sensors. The first type is a relative humidity/ temperature sensor. Six of the relative humidity/temperature sensors were embedded along the beam at different depths. In addition to the RH/Temp sensors, a remote wireless resistance pin sensor was installed on the surface of the beam and monitored over the same period. As a control reference, the beam was weighed continuously over the 60-day period to obtain a theoretical moisture content.

The results indicate that the moisture content recorded by the sensors varied with the depth of the sensor. In addition, the sensors were limited in the upper range to the fiber saturation point. The beam started with a moisture content of approximately 75% and the fiber saturation point is approximately 25%; therefore, the sensors did not provide meaningful data until the moisture content was below 25%. The study provided preliminary work with regard to the development of wood moisture sensors, offering a starting point for future work.

1.4.4 Demonstration of a Fibre-Optic Sensing Technique for the Measurement of Moisture Absorption in Concrete (Yeo et al. 2005)

In this study, a fibre-optic-based humidity sensor was developed and used for the measurement of moisture absorption in concrete. The humidity sensor used in this work was based on expansion principles, using a fiber Bragg grating (FBG). The humidity sensor was created by coating an optical fiber containing an FBG with a moisture-sensitive polymer that absorbs the moisture, causing it to swell. This swelling stretches the fiber and causes a strain in the FBG. This process changes the wavelength of the reflected signal which can be monitored using an optical spectrum analyzer or any other similar wavelength-based interrogation technique.

To fabricate the sensors used in this work, the fiber optic first had a fiber Bragg grating (FBG) written in B/Ge co-doped photosensitive fibers using the phase mask technique. The FBG samples were then annealed at 200^{o}C (392^{o}F) for seven hours and then treated with a silane coupling agent prior to the coating. A multiple dip coating process involving 20 layers was used to coat the FBG with polyimide.

Protection of the sensor was a concern due to the fragile nature of the fiber and the need to use it as a probe. Protection was achieved by using a thin metal tube to cover the sensor and having holes drilled along each side to allow the free circulation of fluids. The metal tube was fixed to the sensor using epoxy resin.

To test the sensors, standardized cylindrical samples of concrete were made with a diameter of 100mm and a length of 100mm. The cylinders were cast with a 4 mm diameter hole at the center to a depth of 80 mm, creating a void for the sensor to rest in. For each test, a sample was set up with the probe placed in the center of a concrete cylinder. The entry point of the probe was then filled with the malleable wax, to prevent any water from seeping in and the room humidity having any effect on the measurements. The sample was left for approximately one hour to allow the sensor to reach equilibrium. Next, the sample was placed in a water bath with a controlled water level and the temperature regulated at 23^{o}C. The characteristic wavelength of the FBG was then determined. The relative humidity was then calculated using a previously obtained calibration chart.

The laboratory results showed that the fiber-optic-based humidity sensors can be used

effectively to monitor moisture changes in different concrete samples. This indicates that there is a potentially new application of the sensor system to ensure the integrity of civil engineering structures in general.

1.4.5 Long-term Monitoring of Timber Moisture Content below the Fiber Saturation Point using Wood Resistance Sensors (Dai and Ahmet 2001)

In many applications, commercial resistance-type moisture meters have their drawbacks, including calibration, polarization, and the constraint of measuring points. In this study, a moisture sensor was designed to meet the stringent requirements with respect to accuracy. The designed sensors, or probes, consist of two pairs of silver-painted brass screw-type electrodes inserted into a wood buffer 13mm apart. These parallel electrodes, equivalent to a network of six resistances, provide the potential for measuring moisture gradients. The probes were tested in Beech samples. The probes were inserted in 10mm diameter holes and sealed to ensure the outside atmosphere did not affect the sensor environment. The results of the study showed that the moisture probe compares well with readings obtained from commercially available moisture meters. Further, the prototype sensor was able to be wired into a data logging system, making the probe ideal for timber applications requiring accurate long-term moisture measurements.

1.5 References

American Standards for Testing Materials.Standard Test Methods for Laboratory Standardization and Calibration of Hand-Held Moisture Meters. 2008.ASTM International, West Conshohocken, PA. ASTM D4444-08.

American Standards for Testing Materials. Standard Test Methods for Direct Moisture Content Measurement of Wood and Wood-Base Materials. 2007.ASTM International, West Conshohocken, PA. ASTM D4442-07.

Dai, G.; Ahmet, K. Long-Term Monitoring of Timber Moisture Content below the Fiber Saturation Point Using Wood Resistance Sensors.2001 Forest Products Journal 51(5):52-56.

Dyken, T.; Kepp, H. Monitoring the Moisture Content of Timber Bridges. Proceedings, International Conference Timber Bridges (ICTB). 2010. Lillehammer, Norway.

Forest Products Laboratory. Wood Handbook: Wood as an Engineering Material. 1999. Madison,WI. 3-5 p.

Wacker, J.P; Joyal, M.R. [and others]. Monitoring the Performance of Timber Bridges over the Long Term. Proceedings, 2007 Mid-Continent Transportation Research Symposium. Ames, IA.

Yeo, T.L.; Eckstein, D; McKinley, B [and others]. Demonstration of a Fibre-Optic Sensing Technique for the Measurement of Moisture absorption in Concrete.2005. Institute of Physics Publishing. 15:N40-N45.

CHAPTER 2 : DEVELOPMENT OF A SMART TIMBER BRIDGE—SENSOR EVALUATION

Modified from a paper to be submitted to *Transportation Research Record: Journal of the Transportation Research Board*

Trevor Pence, Brent Phares, Ursula Deza, Jim Wacker

Abstract

To date, timber bridge evaluation and maintenance efforts utilize non-destructive evaluation tools and visual inspection data to determine the structural integrity of timber structures. This work is part of a comprehensive effort to develop an innovative smart timber bridge structure capable of monitoring long-term performance parameters. The smart timber bridge system is intended to improve the long-term performance, maintenance, and management of timber bridges. In this paper, timber-specific sensors capable of measuring structural adequacy and decay/deterioration are evaluated for accuracy and survivability. A technique to embed and attach strain gages within glued-laminated timber girders was developed and tested on a full-scale. Additionally, various moisture sensors were assessed with the purpose of detecting decay/deterioration in timber bridge components. The timber-specific sensors developed in this work continue the development of a smart timber bridge.

2.1 Introduction

The critical deterioration of bridges nationwide has initiated the search for new methods to rehabilitate, repair, manage, and construct bridges. As a result, smart structure concepts have emerged as a new technology to help improve future bridge management. The idea is to develop and deploy civil systems that have sensors integrated into them such that the condition and performance of the system can be reported on continuously and, generally, remotely. The smart structure approach could potentially replace or supplement the on-site inspections currently specified by the National Bridge Inspection Standards (NBIS). In the case of timber bridges, traditional condition assessments have been determined by visual inspection and basic testing of the structure's members with maintenance decisions being based upon the gathered information. To improve this situation, the development of an innovative timber bridge structure with capabilities to monitor long-term performance parameters was undertaken as part of a previously developed Five-Year Research Plan (Phares et al., 2010).

The objective of the Smart Timber Bridge Research Plan is to develop smart timber bridge structures by utilizing existing and novel forms of instrumentation, health monitoring technologies, and bridge management approaches to develop one turnkey Structural Health Monitoring (SHM) system. Four broad needs were established for the development of the smart timber bridge comprising of:

- Selection of the bridge structure materials
- Identification of the measured parameters
- Selection and development of sensor types
- Data processing and reporting

Structural glued-laminated timber (glulam) was selected as the principal material for the smart timber bridge components. Glulam is an engineered, stress-rated product that has recently grown in popularity due to several distinct advantages including: size capability, architectural effects, seasoning, variation of cross sections, grades, and effects on the environment (Wood Handbook, 1999). The development of the smart timber bridge will

focus on superstructure components consisting of a series of transverse glulam deck panels supported on longitudinal glulam beams.

The condition assessment of the smart timber bridge will be conducted through evaluating structural adequacy and deterioration/decay. The structural adequacy will principally be evaluated by measuring flexural strains to determine changes in stiffness of the bridge superstructure. In addition, deterioration/decay will be assessed through commercially available timber moisture sensors.

One important step in the smart timber bridge developmental research plan is to develop data processing techniques and software applications to interpret and report the results from data obtained during monitoring periods. The condition of the bridge is then presented to the bridge owner in a clear report. With this information, the owner could program routine maintenance and/or rehabilitation to the bridge.

To date, bridges constructed with glulam have received minimal attention from the broad health monitoring community; thus, long-term in-situ behavior is not well understood.

Moisture plays an important role in determining the life of wood and is known to facilitate several deterioration processes (Wood Handbook, 1999). Moisture can both reduce the decay resistance of wood and can cause severe degradation of the material properties. Also, it is known that moisture can accelerate fatigue life usage in compression members. Currently, several techniques to evaluate moisture are used during regular inspections. However, most bridges are inspected once every two years; thus, deterioration due to moisture may not be identified immediately. A program that monitors moisture continuously is a critical need if early decay/deterioration are to be detected.

Previous work to develop a timber bridge moisture monitoring program has been attempted. Dyken et al. instrumented five Norwegian timber bridges with relative humidity/temperature sensors to observe changes in moisture content (Dyken et al., 2010). Results from field and laboratory testing showed that moisture contents varied significantly with changes in wood temperature. As a result, the researchers developed a new equilibrium moisture content (EMC) formula that has less dependence on temperature variations. The Forest Products Laboratory (FPL) conducted a preliminary study to monitor the performance of timber bridges over the long-term (Wacker et al., 2007). Relative humidity/temperature

sensors and remote wireless resistance pin sensors were installed on a birch beam specimen. The results show that the moisture content varied with the penetration depth of the sensors; furthermore, the sensor measurements were limited up to the fiber saturation point. Dai et al., developed a novel timber moisture sensor with the purpose of achieving improved accuracy (Dai et al., 2001). The designed sensors consist of two pairs of silver-painted brass screw-type electrodes inserted into a wood buffer. The sensors were tested in a Beech sample and the results compared well with commercially available moisture meters. Further, the sensors could be wired into a data logging system, making it ideal for SHM applications.

The initial part of the Smart Timber Research Plan focused on integrating fiber optic strain sensors, using Fiber Bragg Grating (FBG) technology, into glulam members to evaluate structural adequacy (Phares, 2010). Structural packages were developed to protect the fragile bare FBG strain sensor during handling and installation while also providing mechanical connectivity between the FBG sensor and the glued-laminated specimen. The structural FBG sensor package conceptually consists of a backing material and a bare FBG strain sensor bonded together. The resulting system could be either attached to an exposed wood surface or embedded between the laminates of glulam members to measure the response of the member to external forces. In this work, five backing material configurations were developed using either stainless steel shims or aluminum mesh sheets shaped as shown in Figure 2. The dimensions of the structural packages were developed to resist the horizontal shear stresses and to allow for the redistribution of localized strain irregularities between the package and the wood laminates. The embedding technique consisted of surface preparation, followed by the application of a structural adhesive to bond the backing material to the wood laminate. After curing for a minimum of 24 hours, the bare FBG sensor was applied to the backing material using a similar structural adhesive and cured for an additional 24 hours.

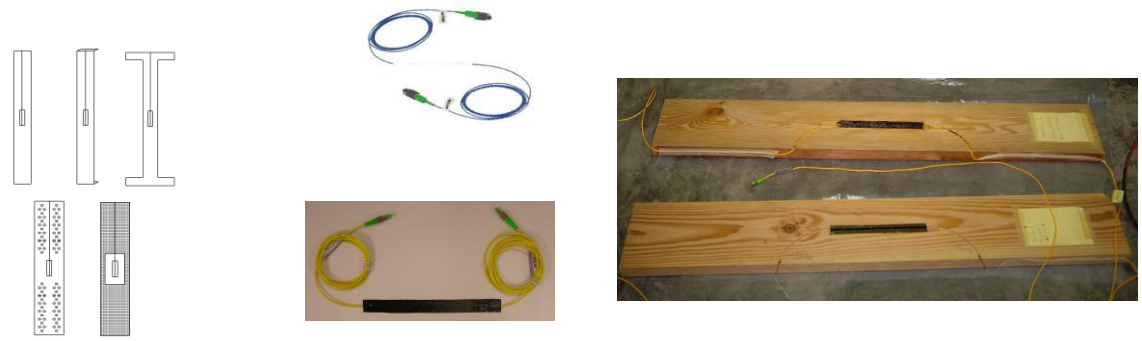

a.) Backing materials b.) FGB strain sensor c.) Instrumented internal wood laminates

Figure 2: FBG Sensor Packages: Materials and Installation

A testing program was conducted on nine small glulam specimens to investigate the adequacy of the sensor packages. A series of bending tests were performed by varying the rates of loading, cycling loadings and sustaining loadings under uncontrolled ambient temperatures as well as imposed heat and cold temperature conditions. Upon completing the small-scale testing, the most promising sensor packages and attachment techniques were selected and implemented in a full-scale glulam girder. The general conclusions from small-scale and full-scale evaluations were:

- Techniques for embedding and attaching FBG sensor packages for structural monitoring in small scale specimens worked adequately immediately after set up. However, the survivability of the sensors decreased when the specimens were released from the assembly fixture and handled for testing. In general, sensor damage occurred at the fragile bare strand transition between the packaged bare FBG sensor and the leads
- The consistent performance of the FBG sensor packages was proven through the reproducibility of the bending strain data while varying the duration of the load. In all cases, minimal strain differences were observed among average strain levels.
- In the full scale glulam girder, an improved installation process and assembly of sensor packages was satisfactory. However, additional manufacturing activities were

found to damage the internal FBG sensors. In this context, the sensor installation technique needs to be improved to be suitable for manufacturing.

2.2 Moisture Sensor Evaluation

Three commercially available moisture sensors were evaluated for survivability and accuracy of measurements for this evaluation. Four 6 in. x 6 in. x 2 in. Southern Yellow Pine (SPY) specimens were tested under varying relative humidity and temperature conditions. All specimens had each of the three moisture sensors discussed herein and shown in Figures 3 and 4.

The first sensor is a relative humidity/temperature sensor (RH/Temp). The moisture content of timber below the fiber saturation point is a function of both relative humidity and temperature of the air surrounding it (Wood Handbook, 1999). Thus, by embedding a RH/Temp sensor in a small void within the timber, an equilibrium moisture content (EMC) can be obtained assuming the moisture content of the wood is in equilibrium with the humidity of the air void within the timber. To embed the RH/Temp sensors, a 1/2 in. diameter hole was drilled 2 1/2 in. deep. Next, a 1/4 in. diameter hole was drilled an additional 1/2 in. to create a void for the sensor to rest in. A 3/8 in. plastic sleeve was inserted to the 2 1/2 in. depth to restrict moisture penetration into the sensor void from other areas of the specimen. The sensor was then inserted into the hole, resting in the void. Silicon sealant was placed over the top of the sleeve to restrict the intrusion of ambient conditions into the sensor void.

The second sensor chosen for evaluation is called a Point Moisture Measurement (PMM) sensor. The PMM sensor measures the electrical resistance between two #6 screws driven into the timber. The electrical resistance is then converted to a moisture content based on an empirical relationship corrected for species and temperature. The PMM sensors were installed by simply driving two #6 3/4 in. screws through the sensor and into the wood. The sensors were orientated such that the screws were aligned parallel to the wood grain direction.

The final sensor chosen for evaluation is called an Embedded Moisture Sensor (EMS). The EMS sensor is used to perform an indirect measurement of moisture levels in materials

not compatible with standard measurement techniques. The sensor is essentially a wooden plug with electrodes attached to each end. The electrical resistance of the plug is measured to determine the relative moisture content of the surrounding area. A similar technique as the RH/Temp sensors was used to install the EMS sensor. A 9/16 in. diameter hole was drilled 3 in. deep and the sensor was inserted to the full depth. The saw dust from the drill hole was used to fill the space from the sensor to the surface. The top of the hole was then sealed with silicone sealant.

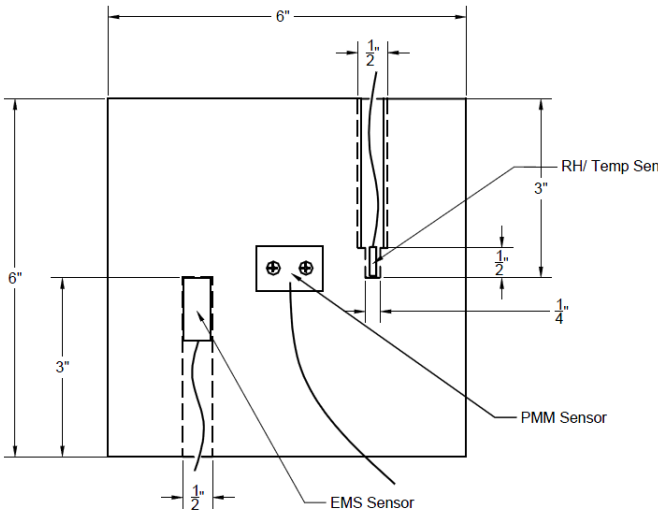

Figure 3: Typical Test Specimen

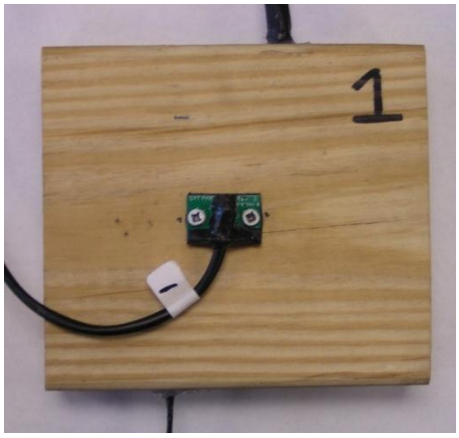

Figure 4: Specimen #1 (Typical of all Specimens)

The specimens were subjected to varying moisture conditions to evaluate the survivability and response of the sensors. All moisture testing was done at the Forests Products Laboratory (FPL) in Madison, WI. First, the four specimens were placed in an environmentally-controlled room with a temperature of 80°F and relative humidity of 90%. These conditions correspond, theoretically, to an equilibrium moisture content (EMC) of 20%. After the EMC was reached, the specimens were placed in a drying room at 80°F and 37% relative humidity until the corresponding EMC of 7% was reached. Lastly, the specimens were placed back in the 20% EMC room. As a reference, the moisture content was periodically checked with a commercially available moisture meter.

Figure 5 illustrates the typical performance of the moisture sensors in all specimens tested as part of this work. The point at which the specimen changed environmental rooms is easily observed by a sudden drop or increase in moisture content. Another obvious trend in the graph is each sensor's moisture content relative to the others. The RH//Temp sensor is consistently higher than the EMS and PMM sensors while the EMS sensor reading is consistently lower than the RH/Temp and PMM sensor.

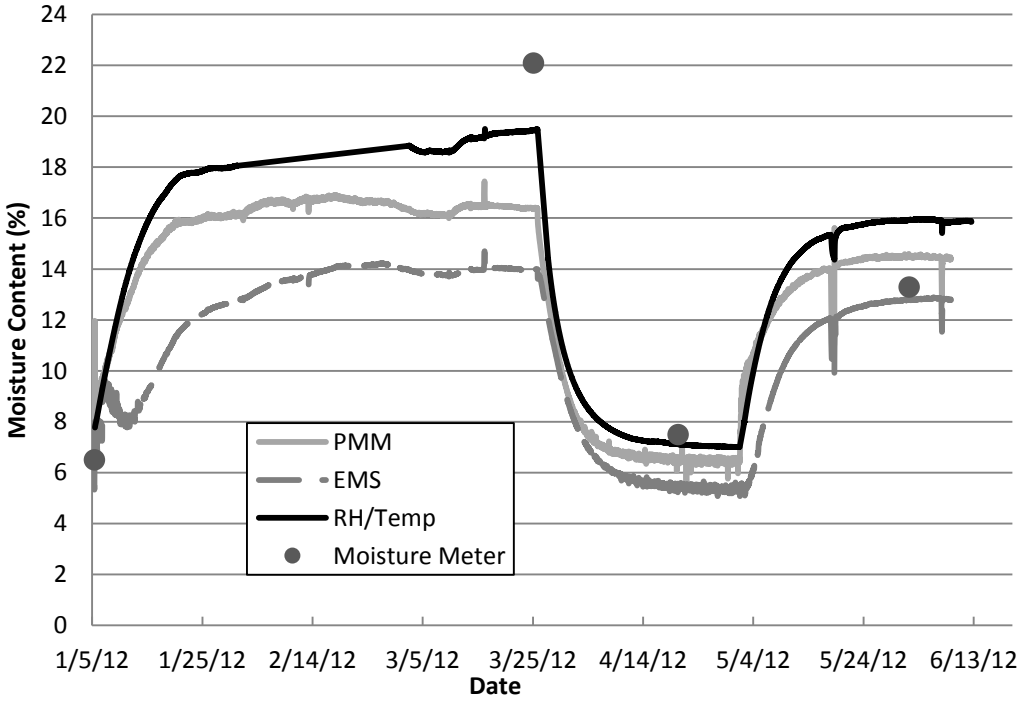

Figure 5: Specimen 1 Results (typical of all specimens)

The RH/Temp sensors appeared to be the most accurate when compared to the moisture meter. The sensor was able to read moisture contents near 20%. The threshold moisture content for incipient decay in wood is around 20%; therefore, accuracy around 20% MC is important. Another advantage of the sensor is that it experiences less noise compared to the other sensors. The graph shows a smooth line with little variation between successive points. Although the sensor has many advantages, one disadvantage of the sensor is its inability to be wired into an off-the-shelf data logging system capable of reading other sensor types.

The PMM sensor appeared to be most accurate at lower moisture content readings. The

sensor was unable to read a moisture content of 20%, falling short by approximately 5% moisture content. The main difference between the readings from the PMM sensor and the moisture meter is insertion depth of the pins. The moisture meter is equipped with insulated pins that measure the electrical resistance only at the tip of the pins. In other words, the moisture content is obtained at the exact location of the penetration depth. On the other hand, the PMM sensors were equipped with non-insulated screws that measure the electrical resistance throughout the whole length of the screw. The manufacturer of the PMM sensor recommends using a nylon tube that goes around the screw just prior to the desired depth of penetration. Furthermore, another difference between readings is caused by grain orientation. According to the manufacturer, readings taken only inches away from each other could differ by 3% to 5% MC. One advantage of the PMM sensor over the other sensors is ease of installation. Predrilled holes and sealing the sensor are not required, saving time and difficulties in field installation.

The EMS performed the worst when compared to the PMM Sensor and the RH/Temp sensor. The sensor was unable to record readings at the 20% MC threshold, falling short by as much as 8% MC. According to the EMS manufacturer, the EMS is usually used in concrete and sandstone materials where a moisture level is a concern, rather than an accurate moisture content of the material.

As a result of the small scale moisture testing, the PMM sensor was chosen as the superior option for the following reasons:

- The sensor was successfully wired into a data logging system capable of reading other sensor types.
- The installation procedure is easier compared to the other sensor types. The sensor does not require predrilling or sealing, thus saving time and difficulties in field installation.
- The sensor responded well to varying environmental conditions, indicating obvious trends in moisture gain or loss.
- Reasonable accuracy was achieved particularly at lower moisture contents. A drawback of the sensor is its inability to accurately measure moisture contents near 20%.

- The rigidity of the sensor makes it unlikely to become damaged under repeated loading.

2.3 Foil Strain Gage Package Development and Evaluation

To increase survivability of the sensors in the glulam fabrication process, electrical resistance type strain gages, also called foil strain gages, were explored as an alternative to the FBG sensors previously discussed. Two methods of attaching foil gages to timber were evaluated. The first method, termed the "Shim Method" is similar to a sensor package developed for the FBG sensors. The Shim Method consists of a stainless steel shim backing material and a conventional foil strain gage. The stainless steel shim is rectangular in shape and has dimensions of 8 ½ in. x 7/8 in. with a thickness of 0.005 in. The second method is termed the "Patch Method". The basic idea of the Patch Method is to apply an adhesive patch, or coating, to the wood surface to fill in any voids or irregularities. The patch cures and a foil strain gage is then applied to the patch using standard strain gage installation procedures.

To evaluate if the Patch and Shim strain gages could be successfully integrated into production type bridge girders, a full-scale beam was designed and constructed at a local glulam fabrication facility. The designed girder represents a single girder from a fictitious double lane timber bridge with a 24-ft roadway width. The fictitious bridge superstructure was assumed to consist of seven 31-foot long glulam girders typically spaced at 44 in. with a cross section of 27 1/2 x 6 3/4 in. supporting a 5 1/8 in. thick transverse glulam deck (Wipf, 2005). The layup of the girder consisted of twenty Douglas-Fir laminates symmetrically balanced in lumber quality and strength through the depth (i.e. 24F-V8 (DF/DF)). In addition, the girder was pressure treated with Pentachlorophenol to evaluate the adherence of the developed strain gages to treated timber.

The locations of the strain gages embedded in and attached to the girder are shown in Figure 6. Additionally, PMM sensors were installed on the beam exterior to evaluate sensor performance on a full-scale specimen under multiple loading conditions.

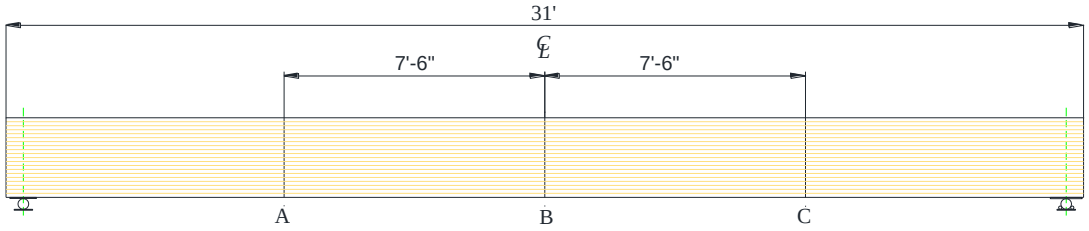

a.) Location along the length

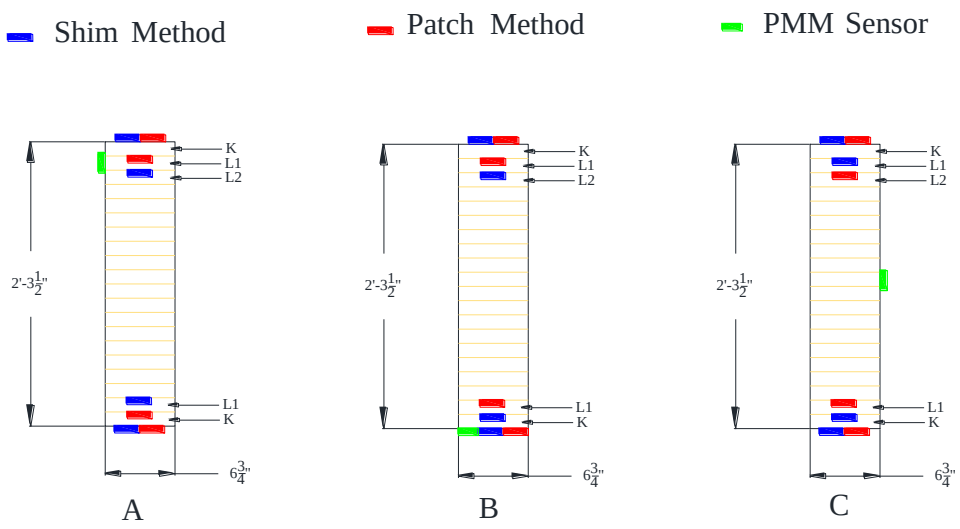

b.) Gage location at cross sections A,B, and C

Figure 6: Gage Location

A typical laminate is illustrated in Figure 7. Three areas along the length of the each laminate are routed 1/4 in. deep, 1 in. wide, and 12 in. long to hold the gages. A groove 1/4 in. wide and 1/4 in. deep is also routed to hold the wires.

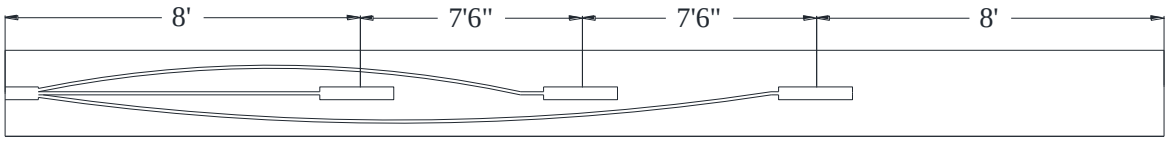

Figure 7: Recessed Areas on a Typical Laminate

The girder was tested under constant amplitude cyclic loads to evaluate the operability of the sensors under repeated loadings. The girder was cycled at a rate of 0.5 Hz for approximately one million cycles with a peak load of 24,000 lbs. The 31-ft girder was supported by one pin and one roller located 6 in. from each girder end. The girder was tested in bending by the two-point loading method as shown in Figure 8. To apply the load at two points, a steel load frame was positioned at midspan and a 10 ft HSS 6 x 6 x 1/4 in. spacer beam was used to transfer the load from the actuator to two points on the beam spaced 9 ft. apart. Further, two inverted T-frames were fabricated and positioned to prevent instability during loading.

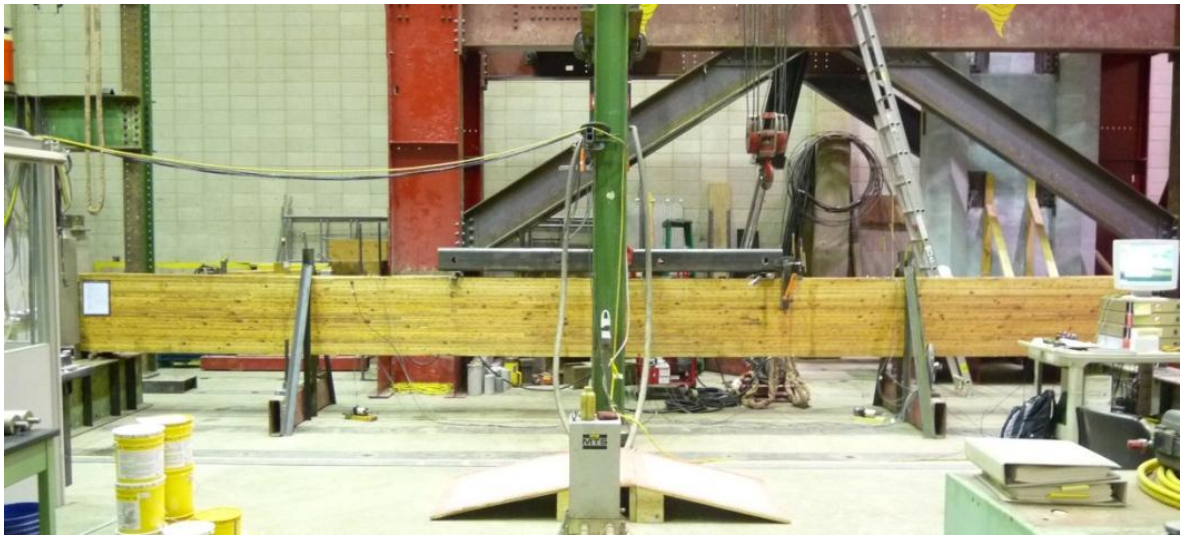

Figure 8: Test Set-Up

2.3.1 Results

Table 2 lists the status of the gages after 1,000,000 cycles. The gages installed using the Shim Method and the exterior Patch Method gages were operable throughout the test; however, the interior gages utilizing the Patch Method were inoperable throughout most of the test.

Table 2--Sensor Performance at 1,000,000 cycles

	Sensor°	Status (O/I)*	Cycles at "failure"	Comments
Shim Method	Top-A	O		
	TL1-A	O		
	K-A	O		
	Bottom-A	O		
	Top-B	O		
	TL1-B	O		
	BL1-B	O		
	Bottom-B	O		
	Top-C	O		
	TL2-C	O		
	BL1-C	O		
	Bottom-C	O		
Patch Method	Top-A	O		
	TL2-A	I	250	No connection
	BL1-A	I	0	Inoperable upon arrival
	Bottom-A	I	0	Damaged during installation
	Top-B	O		
	TL2-B	I	2,000	No connection
	K-B	I	0	Inoperable upon arrival
	Bottom-B	O		
	Top-C	O		
	TL1-C	I	32,000	No connection
	K-C	I	1	No connection
	Bottom-C	O		

° sensor designation (e.g. TL1-A: Top Laminate L1-Section A)
* Operable/Inoperable

After testing was completed, the girder was deconstructed and the interior gages examined. All the interior Patch Method gages failed in the same manner. The fragile connection between the wire and the gage failed for various reasons. One reason for the gage failure was the lack of stress relief on the gage/wire connection. The gage and wire/gage connection was coated with polyurethane for protection. The polyurethane coating adhered the connection to the wood, inducing stress on the connection under loading. Furthermore,

the interior gages did not come pre-wired; therefore, the wires had to be soldered to the leads on the gage to establish the connection. The exterior gages came pre-wired and the gage/wire connection was relatively less fragile compared to the soldered connection on the interior gages. In short, the lack of stress relief on the gage and a fragile soldered connection led to the gage failure.

2.3.1.1 Strain Response and Comparison

Figure 9 illustrates the typical response of the operable gages. As shown in the figure, some of the gages did not recover to zero strain. This behavior is known as "drift" and is common in foil strain gages. When drift is present, the strain range should be evaluated instead of peak strain. The strain range in this case was calculated by subtracting the minimum strain from the maximum strain per cycle. The consistency of the strain range indicates the gages survived the fatigue loading. Furthermore, the constant strain range implies no beam stiffness loss occurred during the loading.

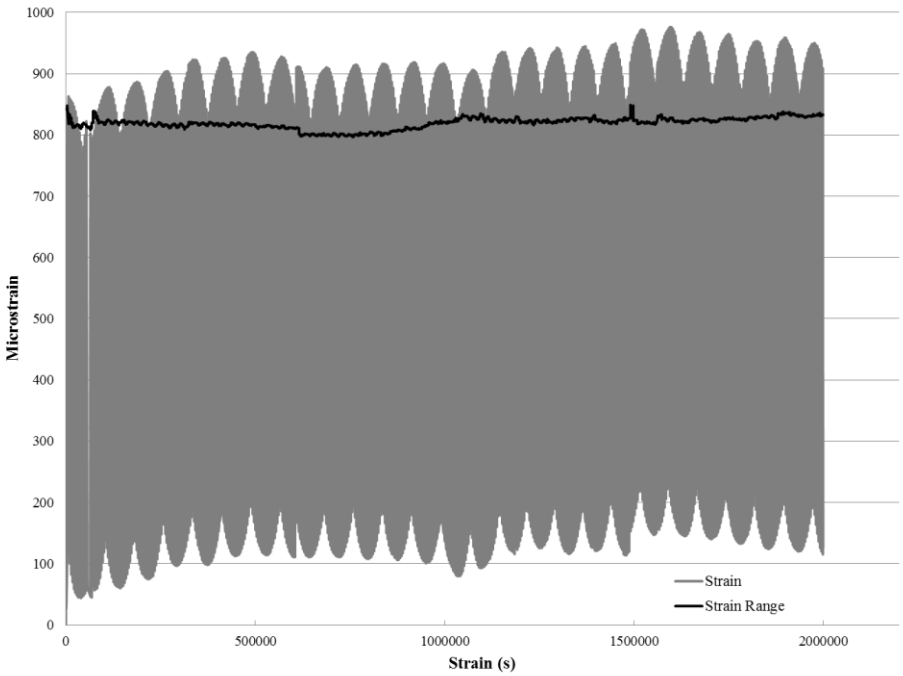

Figure 9: Bottom-A-Shim Strain Range

The peak strain ranges from the exterior Shim and Patch Method gages were compared to observe any differences (see Table 3). The percent differences between gage types ranged from 1.5 to 18.4%. In addition, the Patch Method gages, overall, recorded slightly higher strains compared to the Shim Method gages with the exception of sensor location Top-C. In general, the two gage types compare reasonably well.

Table 3: Exterior Patch Method and Shim Method Strain Comparison

Sensor Location	Shim Gage Average Strain Range (microstrain)	Patch Gage Average Strain Range (microstrain)	Percent Difference (%)
Top-A	512	606	18.4
Bottom-A	819	NA	--
Top-B	811	865	6.6
Bottom-B	867	948	9.4
Top-C	638	628	1.5
Bottom-C	645	710	10.0

Note: NA--Gage damaged during installation

2.3.1.2 Theoretical Strain Comparison

According to the published graded 24F-V8 DF/DF girder characteristics for loads applied perpendicular to the wide faces of the laminations, the modulus of elasticity (MOE) was estimated to be 1800 ksi. Thus, theoretical peak strains were calculated using basic beam theory formulas, assuming that the girder is loaded in the elastic range and both compressive and tensile flexural properties are the same. In Table 4, the estimated strains at each operable gage location are compared to the experimental strains. The percent differences range from minimal to 27.4%. Furthermore, the experimental peak strains are consistently lower than the theoretical values.

Table 4: Theoretical vs. Experimental Peak Strain

	Sensor	Theoretical Peak Strain (microstrain)	Experimental Peak Strain (microstrain)	Percent Difference (%)
Shim Method	Top-A	705	512	27.4
	TL1-A	622	564	9.3
	K-A	686	685	0.1
	Bottom-A	705	819	16.1
	Top-B	987	811	17.9
	TL1-B	871	803	7.8
	BL1-B	808	769	4.8
	Bottom-B	987	867	12.2
	Top-C	705	638	9.5
	TL2-C	584	437	25.1
	BL1-C	611	604	1.1
	Bottom-C	705	645	8.5
Patch Method	Top-A	705	606	14.1
	Top-B	987	865	12.4
	Bottom-B	987	948	4.0
	Top-C	705	628	11.0
	Bottom-C	705	710	0.7

2.3.1.3 Experimental Neutral Axis

At the three cross sections, the position of the neutral axis based on the exterior gages was observed through the fatigue test. The neutral axis position stayed fairly consistent throughout the fatigue testing; however, the neutral axis position did not coincide with the geometrical center of gravity (i.e. 13.75 in). At midspan, the neutral axis location was approximately 0.5 in. above the center of gravity. The difference is attributed to the orthotropic nature of wood.

2.3.1.4 Overload Test

To study the behavior of the sensors under high strains, the girder was loaded to almost double the load used during fatigue testing (i.e. 44 kips). This testing allowed for evaluation of the static performance under overload conditions.

The operable gages at the end of the fatigue test were still functioning at the end of the overload test. The stress-strain plot of the exterior Shim and Patch gages is shown in Figure 10. As shown, the gages demonstrated linear elastic behavior throughout loading. In addition, the modulus of elasticity (MOE) was determined by plotting a linear regression trend line. The MOE ranged from 1466 ksi to 1802 ksi; furthermore, the compressive MOEs were higher than the tensile values.

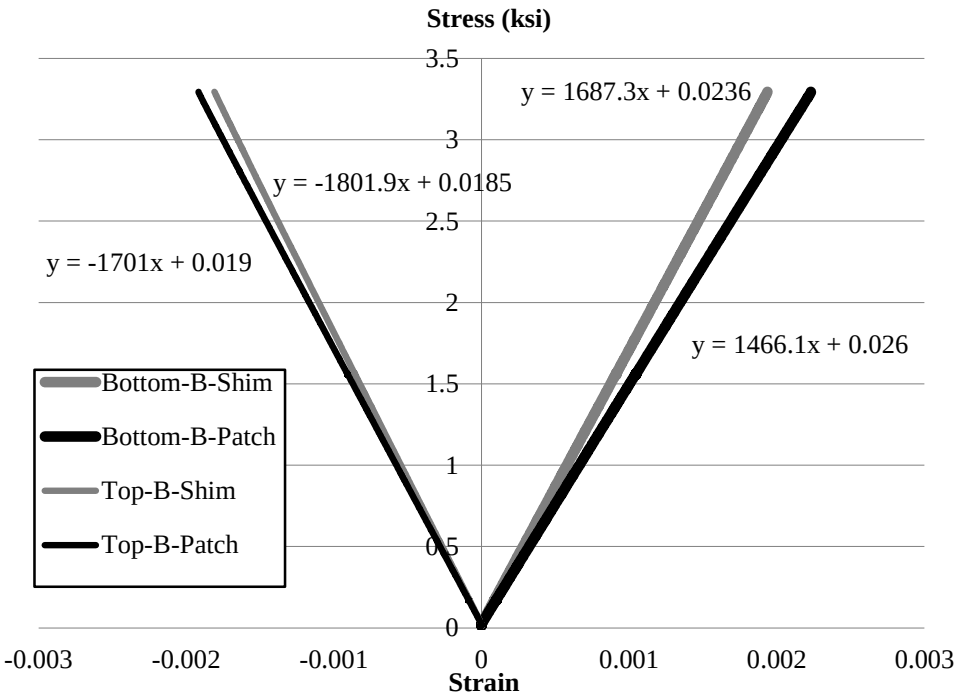

Figure 10: Section B Stress-Strain Plot

2.3.1.5 Moisture Results

Figure 11 shows the moisture content versus time for data obtained from the PMM sensors. In addition, the plot shows the moisture content readings obtained from a conventional moisture meter at the beginning and end of testing. According to the PMM sensors, the initial moisture content of the girder ranged from 9.4% to 10.7%. The moisture content gradually reduced to a range of 7.2% to 8.5% by the end of the test. The EMC corresponding to the room conditions (i.e. 69°F and 40% RH) is 7.7%.; therefore, a reduction in moisture content is expected because the girder is drying out to establish equilibrium with the environment. Furthermore, the PMM sensors consistently recorded moisture contents below the readings obtained from the moisture meter. However, the moisture meter did follow the same trend as the PMM sensors.

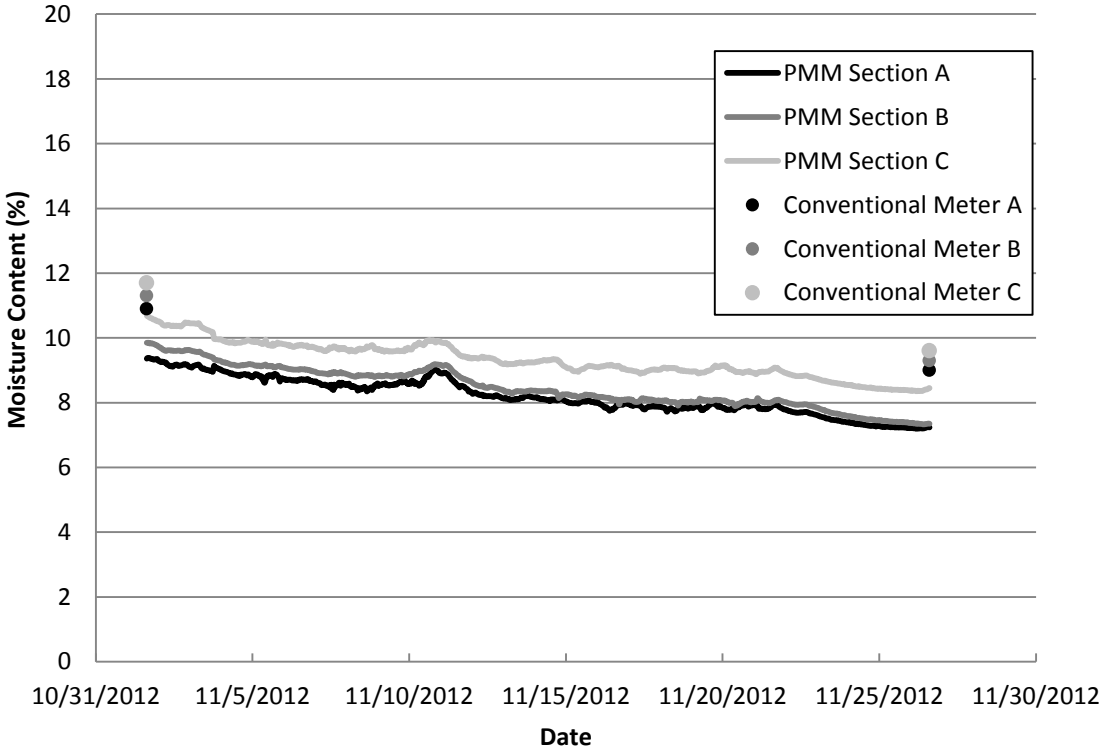

Figure 11: Changes in Moisture Content during Fatigue Test

2.4 Conclusions

This work evaluated potential sensors to be used in the smart timber bridge concept. Overall, the sensors provided reasonable accuracy and exceptional survivability under repeated loadings and overload conditions. In addition, implementing the sensors into the glulam fabrication process proved to be successful.

The general conclusions of the study are:

- The PMM sensor was determined to be the most suitable moisture sensor for the smart timber bridge due to its reasonable accuracy, survivability under repeated loading, and ability to be wired into a data logging system.
- Two methods for attaching and embedding foil strain gages to timber were developed (i.e Shim and Patch Method). Both methods were successfully integrated into the glulam manufacturing process.
- During the fatigue test, both gage types validated each other by measuring similar strains. In addition, the strains were higher than predicted values; however, this can be attributed to difficulties in estimating the MOE in timber.
- The strain ranges of the Shim and Patch Method gages were consistent throughout the fatigue test. Furthermore, the gages were operable after the overload test. Therefore, a conclusion is made that repeated loads as well as overloads do not cause damage to the gages.

The results indicate that the PMM sensor and both Shim and Patch gages are capable of evaluating the structural performance of the smart timber structure. This capability will enable the development of performance based decay/deterioration algorithms.

2.5 References

Dai, G.; Ahmet, K. Long-Term Monitoring of Timber Moisture Content below the Fiber Saturation Point Using Wood Resistance Sensors. 2001. Forrest Products Journal 51(5):52-56.

Dyken, T.; Kepp, H. Monitoring the Moisture Content of Timber Bridges. Proceedings, International Conference Timber Bridges (ICTB), 2010. Lillehammer, Norway

Forest Products Laboratory.Wood Handbook: Wood as an Engineering Material. Madison,WI. 1999.

Phares, B.M., Wipf, T.J. and Deza. U.. Evaluation of Techniques for Embedding and Attaching FBG Sensors to New Glulam Bridge Members. 2010. Bridge Engineering Center; Iowa State University. Ames, IA.

Wacker, J.P; Joyal, M.R. [and others]. Monitoring the Performance of Timber Bridges over the Long Term. Proceedings, 2007 Mid-Continent Transportation Research Symposium. Ames, IA.

Wipf, T.; Phares, B. A 5-year research plan for the development of a smart glue-laminated timber bridge. 2005. Ames,IA: Iowa State University, Bridge Engineering Center

CHAPTER 3 : DATA PROCESSING TECHNIQUE TO DETERMINE CHANGES IN STRUCTURAL STIFFNESS

Modified from a paper to be submitted to *Transportation Research Record: Journal of the Transportation Research Board*

Trevor Pence, Brent Phares, Lowell Greimann, Jim Wacker

Abstract

Recently, efforts have been made to improve bridge management by developing structural health monitoring techniques and approaches. By using conventional sensors and robust data processing algorithms, bridge owners are provided with more timely information on structural performance parameters and maintenance needs. In the case of timber bridges, traditional evaluation and maintenance efforts have been determined by visual inspection and basic testing of the structures members. To address this, a SHM system was developed to continuously monitor timber bridge performance parameters to detect changes in structural stiffness. The proposed system using statistical control chart techniques to observe changes in distribution factors and neutral axis locations. The effectiveness of the system was demonstrated by collecting, reducing, and analyzing ambient strain data from a demonstration timber bridge.

3.1 Introduction

Early detection of damage/deterioration continues to be a goal for bridge managers. The ability to detect damage at an early stage can reduce costs and downtime associated with repair. In the case of timber bridges, traditional condition assessments have been determined by visual inspection of the structure's members with maintenance decisions being based upon gathered information. To improve this situation, a goal was established to develop a smart timber bridge that improves the long-term performance, maintenance, and management of timber bridges.

This paper describes a structural health monitoring (SHM) system that was developed to assess structural stiffness changes in timber bridges. The concept uses statistical evaluation methods to determine changes in structural integrity. The developed system uses strain measurements acquired from ambient traffic to determine live load distribution factors and neutral axis locations. The distribution factors and neutral axis locations are evaluated by applying control chart analysis techniques to determine if the process is in control. A typical control chart uses the mean and standard deviation of measured parameters to establish upper and lower control limits on the process. As an example, parameters falling outside the control limits indicate an out of control process, implying a change in the bridge.

A limited amount of research has been done on long-term monitoring of timber bridges. Moore et al. developed a laser based technique to provide a low cost measurement system that could be easily retrofitted to both old and new structures (Moore et al., 2010). The developed system measures midspan deflections to evaluate timber girder performance. The researchers sampled 300 vehicles with known gross weights and measured their corresponding midspan deflections. Threshold deflections were then established, providing a basis for future ambient traffic. Dyken and Kepp instrumented five Norwegian timber bridges to monitor the moisture content over time. The system proved to effectively measure changes in moisture content; however, the structural response of the bridges was not evaluated (Dyken, 2010).

An extensive amount of SHM research has been conducted on steel bridges. Lu et al. developed a SHM system that autonomously collects, reduces, analyses, and determines damage occurrence in a near-real-time fashion (Lu, 2008). Data processing involves

statistical control chart analysis to detect damage. The system was able to successfully detect damage on a sacrificial specimen attached to an in-service bridge. Bhattacharya et al. monitored peak strains from ambient traffic to determine bridge load ratings. The uses of site-specific data allowed for the removal of uncertainties in live load characterization, resulting in more accurate bridge ratings (Bhattacharya, 2005).

3.2 Bridge Instrumentation and Monitoring System

To demonstrate the developed SHM system, a two-span, glued-laminated, timber girder bridge located in Delaware County, IA was selected for evaluation (Figure 12). Both spans of the bridge consist of six 38 ft. simply supported glued-laminated timber girders. The girders are Southern Yellow Pine (SYP) constructed with a 24F-V3 layup. The girder cross sections are 10 ½ in. by 31 5/8 in. The deck consists of transverse glued-laminated timber deck panels with a 3 in. asphalt wearing surface. The bridge is located on a low-volume gravel county road; thus, vehicles do not normally travel in the typical traffic lanes. The transverse position of vehicles is accounted for in the SHM system.

(a)

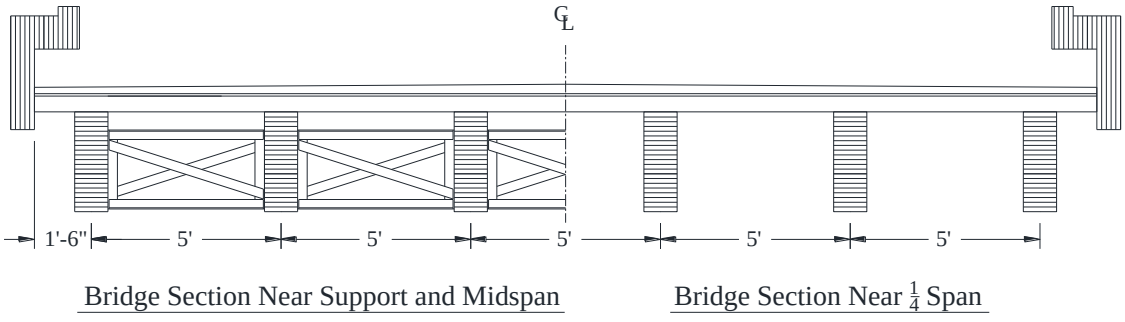

(b)

Figure 12: Demonstration Bridge. (a)Profile View (b) Cross Section

3.3 Hardware System

Figure 13 illustrates the schematic of the SHM hardware system. A data logger reads the raw data from the sensor network and converts the signals into strain or moisture content. The data are temporarily stored on the on-site computer and then sent off-site to an office server via cellular technology. Currently, the entirety of the collected data are sent to the office server. In the future, on-site data processing will occur (e.g. data zeroing, data filtering, and truck detection) before the data are transmitted to the office.

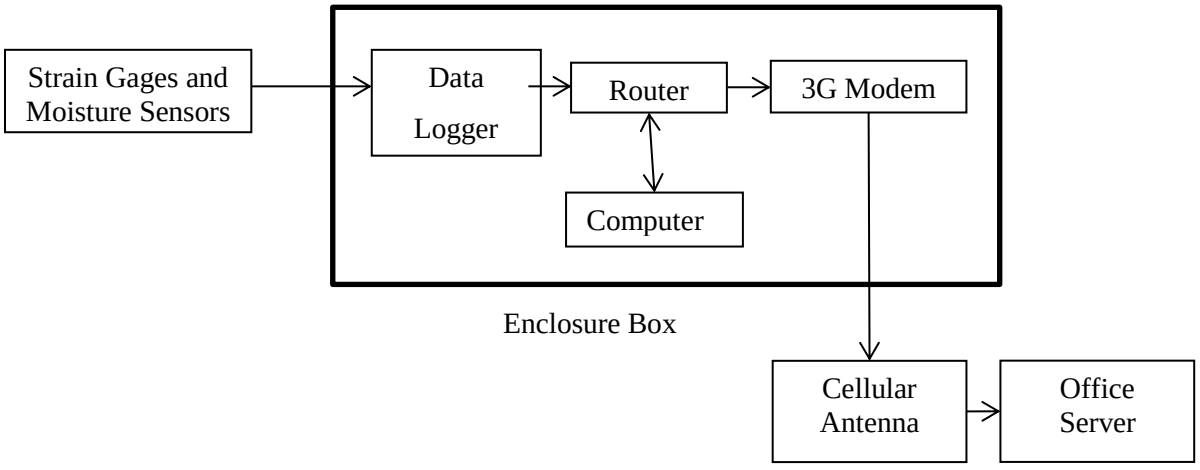

Figure 13: SHM System

The strain gages used in this work were previously developed and tested by the Iowa State University Bridge Engineering Center and the Forrest Products Laboratory (Figure 14) (Phares et al., 2013). The strain gage conceptually consists of a stainless steel shim backing material that account for the variability of the wood surface. The dimensions of the shim were designed to resist the shear stresses and to allow for the redistribution of localized strain irregularities.

Figure 14: Strain Gage

The instrumentation configuration used for the demonstration bridge is illustrated in Figure 15. Thirty four strain gages were installed on the south span of the bridge. Each sensor was assigned a label that designates its location. A two term sensor designation was used to define the longitudinal and transverse location of the girder gages (shown in blue and red). For Example, S-G1 defines the strain gage on girder 1 (G1) at the south abutment (S). The gages at midspan were labeled MT and MB to distinguish between midspan top (MT) and midspan bottom (MB). The deck gages (shown in purple) were labeled with a two term designation. For example, B1-MS defines the deck gage at midspan (MS) in bay 1 (B1).

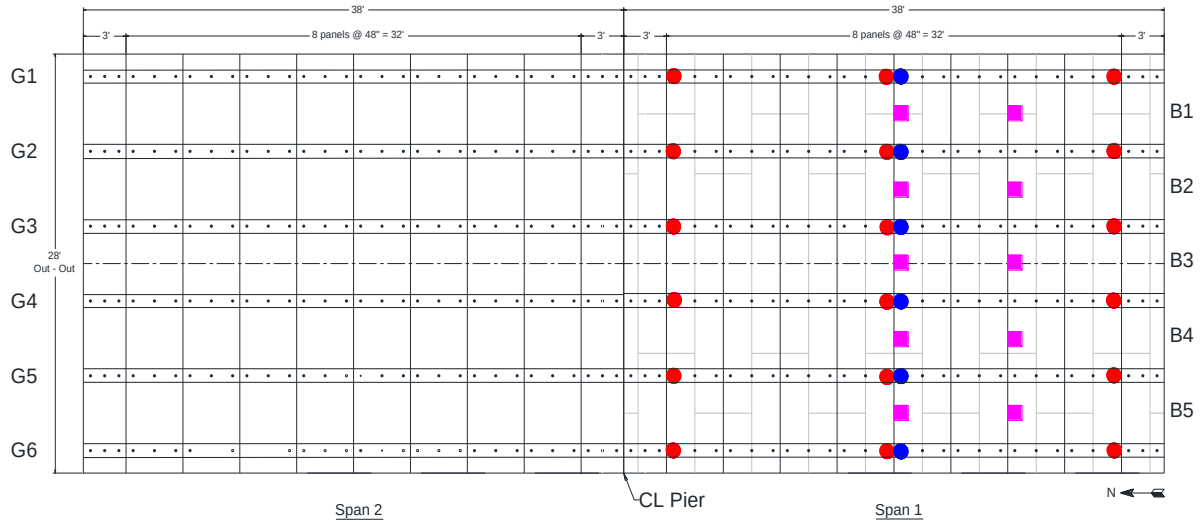

Figure 15: Instrumentation Layout

3.4 Strain Data Collection and Processing

The system records strains at 75 Hz and collects data continuously (i.e. 24 hours a day, 7 days a week). Once per minute a data file is stored and sent to the office server via cellular technology. Recall the bridge is located on a low-volume county road; thus, the majority of the data files do not contain a truck event. In order to avoid manually searching through several data files for truck events, a basic program was written to zero and identify data files that include a truck event. First, the program zeros each individual data file to remove temperature effects and gage drift. A baseline strain value is determined by calculating the mode strain in the data file. The data are zeroed by subtracting the base line value from the raw data value. Next, gages MB-G3 and MB-G4 are used as trigger gages to identify truck events . The program will search through the data and keep the files with trigger gage readings above 25 microstrain. The 25 microstrain threshold was established to ignore light passenger vehicles. Figure 16 represents the raw and zeroed data from gage MB-G4.

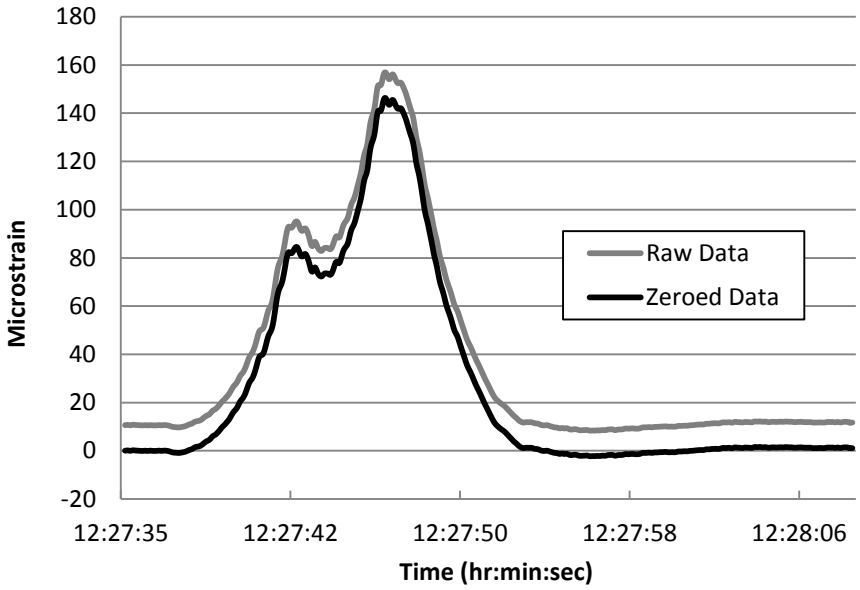

Figure 16: An Example of Raw and Zeroed Data

3.5 Live Load Distribution and Neutral Axis Location

A distribution factor (DF) described herein is defined as the strain value of a particular girder divided by the sum of the strains in all six girders. For each truck event, a DF for each girder is calculated using peak midspan strains. Peak strains are used to maximize the strain response as inherent error occurs at low strain levels. A load test was conducted to observe changes in DFs with respect to transverse truck position. Figure 17 shows the DFs plotted for a truck traveling in the west lane, east lane, and center of the road way. The figure shows that girders directly under the lane the truck is traveling in receive the most load. On the contrary, girders further from the loaded lane receive less load.

One could look at the distribution factor plot to determine which lane a particular truck is traveling in. However, if a girder becomes damaged or loses structural integrity, utilizing girder strains to determine lane position is no longer a valid assumption. To address this, gages were installed on the underside of the deck to determine the transverse truck location. The transverse position of a truck is identified as east, west, or center. Load tests conducted on the demonstration bridge have shown that deck-bottom gages near the truck wheel lines produce strain peaks that correspond to the truck axles. Figure 18 illustrates the strain

response from deck-bottom gages during a center load path. Since the girder spacing is only 5 ft. and typical truck wheel lines are spaced at approximately 7 ft, the wheel lines of a center truck event are located in B2 and B4. Therefore, gages in B2 and B4 produce peak strains that correlate to the axles. As such, truck events that produce peak strains in B2 and B4 that clearly define the truck axles are identified as a center event.

The majority of vehicles were observed to have travelled in the center of the bridge. As a result, the trucks travelling in the east and west are ignored due to a small sample size. Note if the SMH system was implemented on a typical highway bridge with more well defined traffic lanes, trucks traveling in the traffic lanes would be considered and trucks travelling in the center of the bridge, outside the traffic lanes, would be ignored.

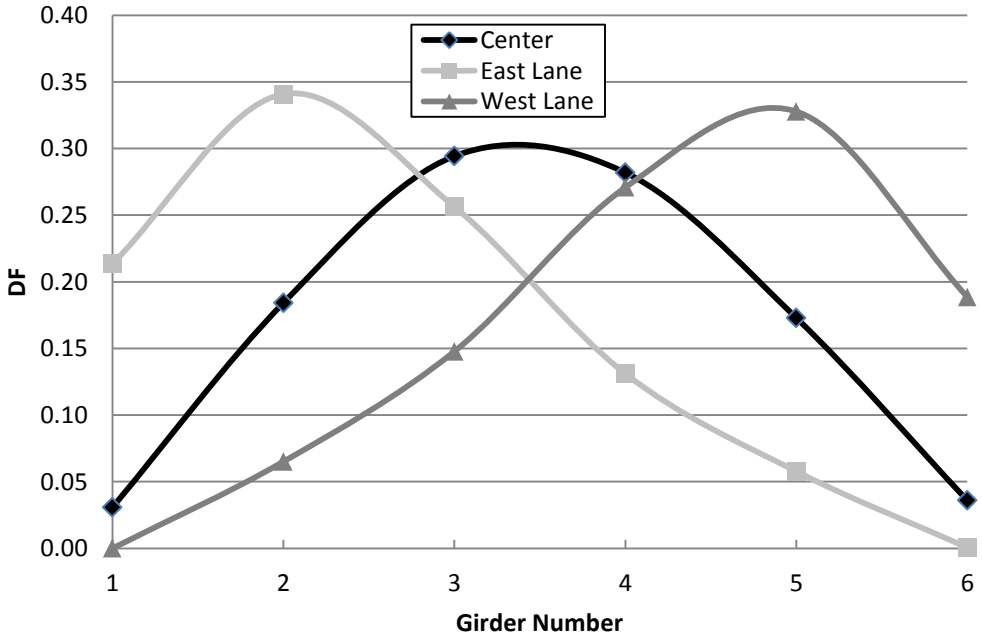

Figure 17: Distribution Factors for Center, East, and West Lanes

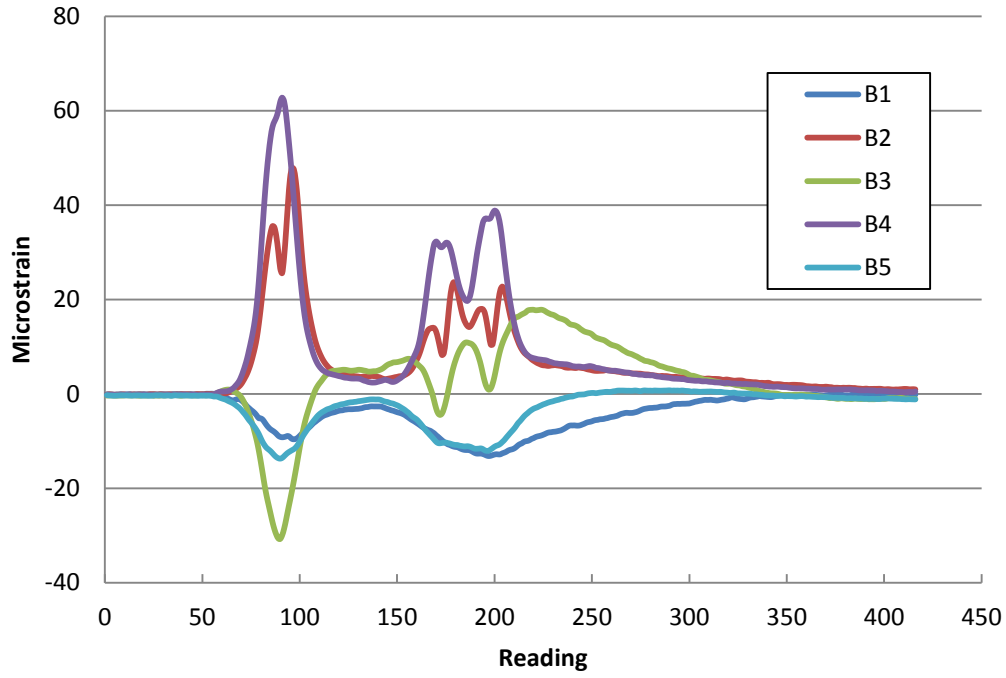

Figure 18: Deck Bottom Strain Response for a Center Truck Event

In addition to DF, monitoring the neutral axis (NA) can provide possible indications of structural stiffness changes. The NA can provide information on the composite action between the deck and girder. Specifically, a reduction in composite action can be observed by a drop in the NA. Furthermore, deterioration of the beam and/or deck can be detected by observing a change in the NA.

The NA is measured from the extreme bottom fiber in Girders 2, 3, 4, and 5. As a general rule, the NA should not be calculated if the difference in top and bottom strain is less than 25 microstrain; therefore, Girders 1and 6 are ignored due to low strain magnitudes.

Figure 19 illustrates how the NA is determined for a typical event. The greatest strain response occurs at midspan where the maximum bending moment occurs; thus, the NA is calculated at midspan. Shown in Figure 19, the NA location at midspan is reasonably consistent as a truck passes over the bridge; however, a sudden peak occurs as a truck axle passes over the midspan gages. This peak is caused by localized strains in the top midspan gages and should be ignored. Load test data has shown that the maximum compressive strain

occurs between axle peaks. As a result, the maximum compressive strain and the corresponding tensile stain are used in the NA calculation. Finally, the location of zero strain (i.e. NA) is found using linear interpolation under the assumption that plane sections remain plane.

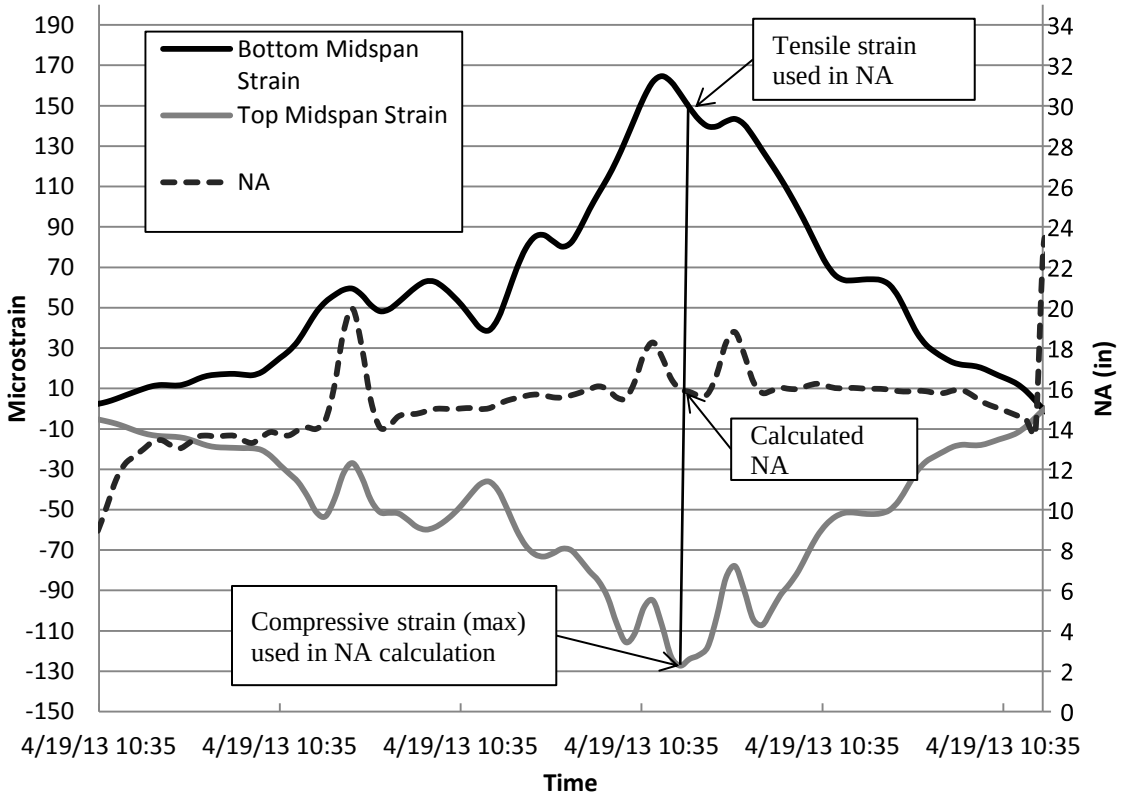

Figure 19: Graph Illustrating NA determination

3.6 Training Period and Control Chart Construction

The developed method uses a training period to establish the control limits of the system. During the training period, an assumption is made that the process is stable; in other words, no change in structural stiffness occurs. Additionally, the data are assumed to be normally distributed. Normalcy was verified by constructing and observing histograms and normal probability plots.

The training period consisted of 100 truck events traveling in the center of the bridge. The 100 truck event period corresponds to approximately 3 months of ambient traffic data collection and is assumed to be an adequate sample size for control chart construction. The range in DFs for all 100 events illustrated in Figure 20 can be attributed to differing wheel line spacing's and slight variations in transverse position (i.e. not exactly center). Further, the NA location for all 100 center lane truck events is shown in Figure 21. The average NA location for each girder is shown by a green line.

.

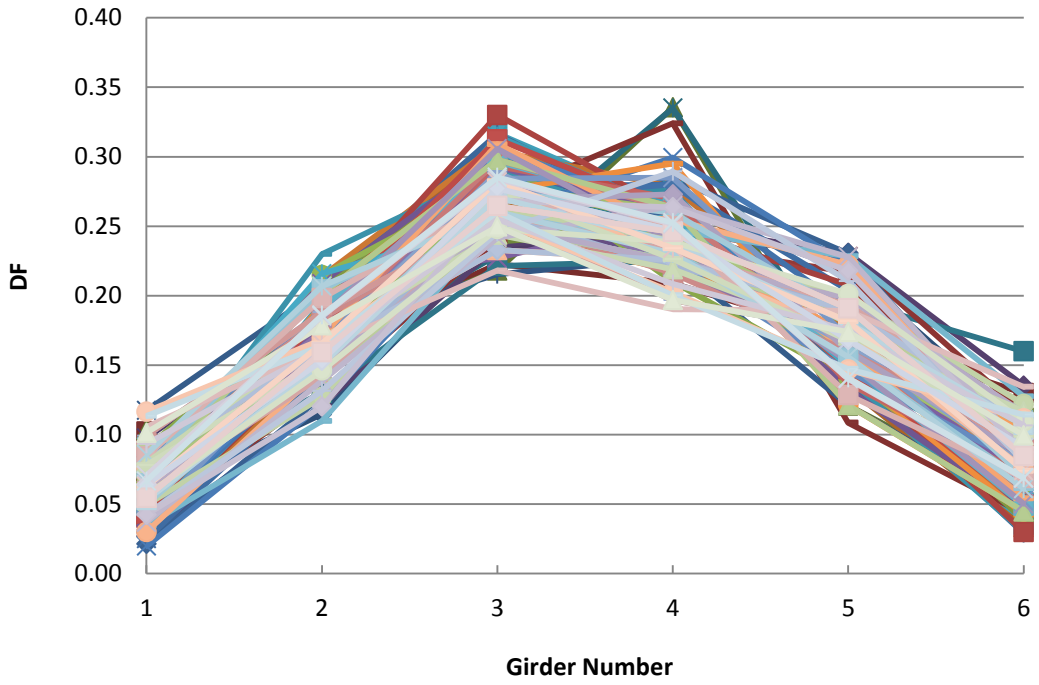

Figure 20: Distribution Factor Range for Center Lane Traffic

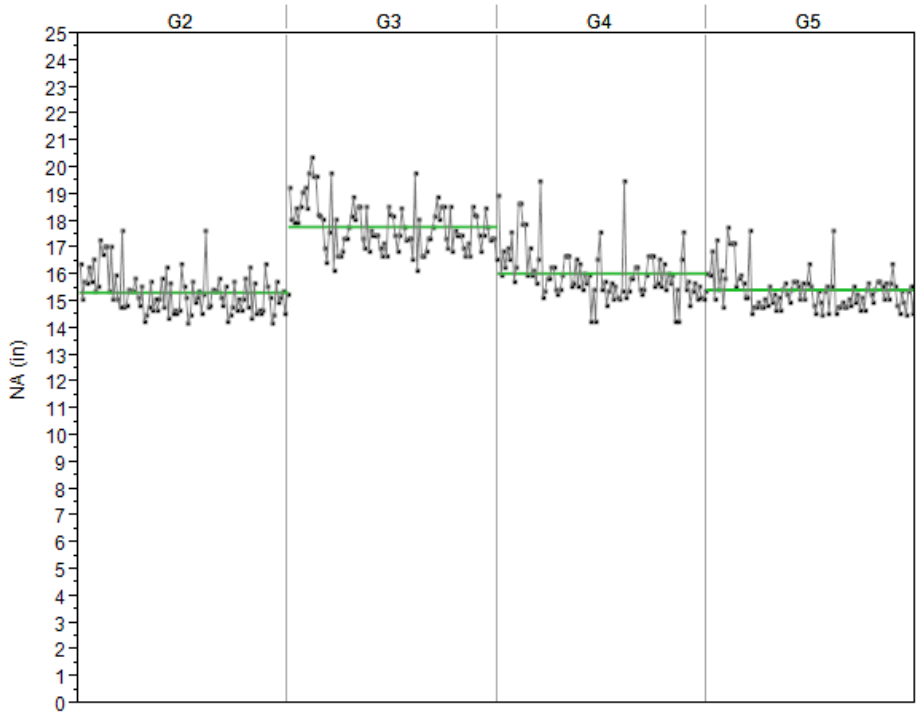

Figure 21: NA Location during the Training Period

The 100 center truck events were further reduced into 20 truck groups (i.e. 5 truck events per truck group) to construct the control chart. This means that data from five center truck events are averaged and represented by a single data point on the control chart. Truck group size is an important parameter that affects the control limits. A large group size generally results in tighter control limits, allowing small variations to be detected earlier. However, by setting the limits closer to the center line, false positive alarms are increased. Previous work suggests using a truck group size of ten (Lu, 2008). However, the truck group size used in this work was reduced to five due to low traffic volumes. Acquiring a truck group size of ten would take several days, thus causing a detection delay in the case of a sudden stiffness change. A truck group size of five is envisioned to detect both short term and long term variations.

The upper and lower control limits of the measured training parameters are found using Equations 3-4 (Vardeman, 2001). The $\bar{s}/c_4$ term is used to estimate the population standard deviation. C_4 is a function of truck group size(m) and increases from about 0.8 when m = 2 to

essentially 1 for large group sizes. A_3 is also a function of truck group size and can be found in tables in most statistical process control text books.

$$LCL = \overline{\overline{X}} - A_3\bar{s} \quad (3)$$

$$LCL = \overline{\overline{X}} - A_3\bar{s} \quad (4)$$

Where:

$\overline{\overline{X}}$ = average of truck group means

$\bar{s}$ = average standard deviation of truck groups

$$A_3 = \frac{3}{C_4\sqrt{m}}$$

m= truck group size

Table 5 shows the established control limits for each girder obtained in the training period. One and two-sigma control limits are found by replacing the "3" in the A_3 term with one and two, respectively.

Table 5: Training Period Distribution Factor Control Limits

	G1 (DF)	G2 (DF/NA)	G3 (DF/NA)	G4 (DF/NA)	G5 (DF/NA)	G6 (DF)
$\overline{\overline{X}}$	0.06	0.17/15.4	0.27/17.8	0.25/16.1	0.17/15.4	0.08
UCL	0.09	0.20/16.3	0.30/18.7	0.28/17.1	0.21/16.2	0.11
LCL	0.04	0.14/14.4	0.24/16.9	0.21/15.0	0.14/14.7	0.05
1-sigma upper	0.07	0.18/15.7	0.28/18.1	0.26/16.5	0.18/15.7	0.09
1-sigma lower	0.05	0.16/15.0	0.26/17.5	0.24/15.7	0.16/15.2	0.07
2-sigma upper	0.08	0.19/16.0	0.29/18.5	0.27/16.9	0.19/16.0	0.10
2-sigma lower	0.04	0.15/14.7	0.25/17.1	0.23/15.3	0.15/14.9	0.06

3.7 Post Training Evaluation

3.7.1 Control Chart Criteria

A set of criteria commonly used in control chart analysis is used to determine if the post-training data are out-of-control. If the data satisfies one of the five sets of criteria, then the process is deemed out-of-control, and the system is alarmed. The criterion includes (Stamatis, 2003).

1. A single point outside 3-sigma limits
2. At least seven consecutive points above (or below) the centerline
3. At least seven upward (or downward) consecutive changes
4. At least two of three consecutive points beyond two standard deviations from the centerline (where both are on the same side of the centerline)
5. At least four of five consecutive points beyond one standard deviation from the centerline (where all 4 are on the same side of the centerline)

Criteria 1 signals an immediate change in the measured parameter and further analysis and/or field inspection should be performed immediately. Criteria 2 and 3 signals a drift in the process average which may be a result from girder and/or deck deterioration. Further investigation is needed and recalculating the control limits may be required. Criteria 4 and 5 provide an early warning of a process shift. Note the probability of a false-positive detection for criteria 4 and 5 is about 2% (Stamatis, 2003).

3.7.2 The Runs Test

Another control chart technique to recognize important signals in a process is termed the Runs Test. A run is defined as a series of consecutive positive (or negative) values. The runs test checks whether the number of runs in a sample is about right for a random series. A long run in the distribution factor above or below the centerline would indicate an increase or decrease in the girder stiffness, respectively. The concept of the runs test is to base a

statistical test on the value of Z under the null hypothesis of randomness. For instance, if the absolute value of Z is greater than 1.96, then the null hypothesis of randomness is rejected at the 0.05 significance level (Stamatis, 2003).

For each truck group (i.e. average of five center truck events, $\bar{X}$) a 1 is associated if $\bar{X} > \overline{\overline{X}}$ and 0 if $\bar{X} < \overline{\overline{X}}$. For example, a sequence of 0's and 1's may be 1, 0, 0, 0, 1, 1, 0, 0, and 1. A run is a consecutive sequence of 0's or 1's; As such, the given series has five runs. The runs test uses the following equations to determine whether five is about the right number of runs for a random series.

$$E(R) = \frac{T+2T_A T_B}{T} \tag{5}$$

$$Stdev(R) = \sqrt{\frac{\left(2T_A T_B (2T_A T_B - T)\right)}{T^2(T-1)}} \tag{6}$$

$$Z = \frac{R - E(R)}{Stdev(R)} \tag{7}$$

Where:

T = number of truck groups (total number of 0's and 1's)

T_A= number of truck groups above the mean (number of 1's)

T_B= number of truck groups below the mean (number of 0's)

R = number of observed runs

If the value of Z is large and positive, then there are too many runs in the process. As a result, a zigzagging behavior would be observed in the control chart. Although the zigzagging behavior causes a statistical concern, it likely does not indicate a stiffness change on the bridge as the parameters are neither increasing nor decreasing. If the Z value is large and negative, there are fewer runs than expected under the null hypothesis of randomness. This condition is of greater concern as fewer runs implies the average girder DF or NA is either increasing or decreasing. Therefore, girders with a large negative Z value will require further investigation.

3.7.3 Post Training Data

For demonstration, 80 center truck events (i.e.16 truck groups) of post-training data were evaluated using the control criterion and the Runs Test. The first 40 center events represent the normal behavior of the bridge and the last 40 events represent a change in the transverse stiffness of the bridge. Specifically, the transverse stiffness of the bridge was altered by removing the midspan cross bracings attached to Girder 3. The DF control chart for all 80 center truck events is illustrated in Figure 22 and the control chart criterion and runs test results are presented in Table 6. The UCLs and LCLs established during the training period are shown in red and $\overline{\overline{X}}$ are shown in green (Figure 22). Furthermore, zones A, B, and C represent the limits based on 1-sigma, 2-sigma, and 3-sigma, respectively. As expected, the first 40 events suggest the process is in-control, providing no indication of a change in structural integrity.

It should be noted that false-positive data points occasionally occur even when no change in the process has occurred (i.e. no change in bridge behavior). As a result, the number of false-positive data points is monitored. The limits on the process may need to be changed if false-positive data points occur more frequently when no change in the bridge behavior is assured.

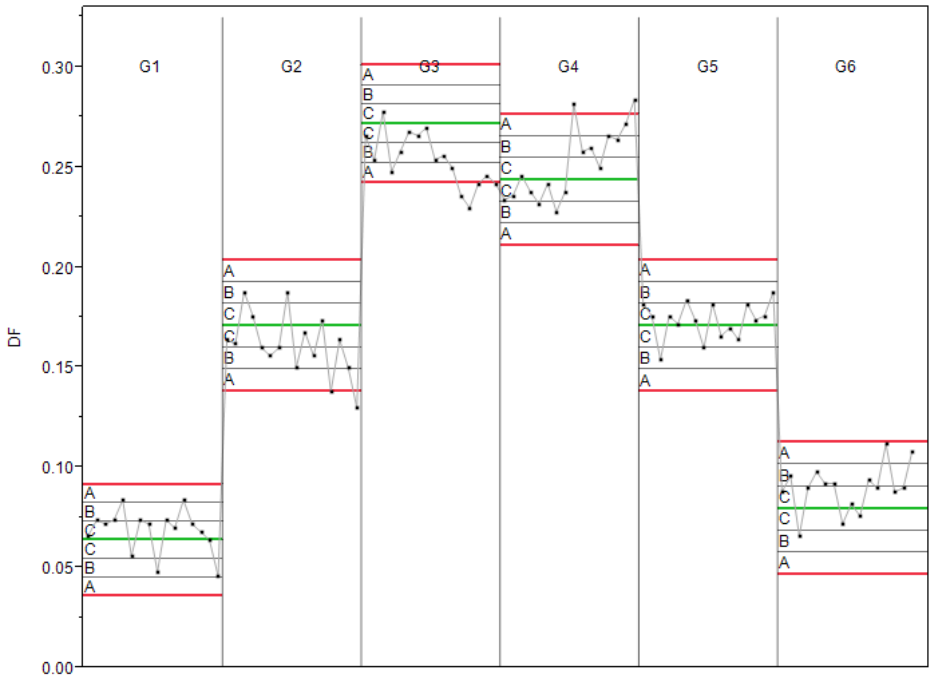

Figure 22: 80 Center Truck Events during Post Training

Table 6: Post-Training Output

		G1 (DF)	G2 (DF/NA)	G3 (DF/NA)	G4 (DF/NA)	G5 (DF/NA)	G6 (DF)
	Runs Test Z-value	-0.70	0 / -1.44	0.33 / 0.58	-2.57/1.03	-0.53/-0.76	1.0
Criteria	1	N	Y/N	Y/N	Y/N	N/N	N
	2	N	N/N	Y/N	Y/N	N/N	N
	3	N	N/N	N/N	N/N	N/N	N
	4	N	N/N	Y/N	Y/N	N/N	N
	5	N	N/N	Y/N	Y/N	N/N	N

*Note: 'N' indicates the critieria was not satified. 'Y' indicates the criteria was satisfied

The data from the last 40 events suggest an obvious shift in the process particularly in Girders 3 and 4. The data suggests the DFs for Girders 3 and 4 satisfy 4 of the 5 control chart criterion, indicating the process is out-of-control. The absolute value of the Z-value in Girders 4 is greater than 1.96; therefore, the null hypothesis of randomness is rejected at the 0.05 significance level. The Z-value of -2.57 is large and negative, implying there are fewer runs in the process than expected. An interesting observation is that the Runs Test did not result in a significant Z-value for Girder 3 when an obvious shift in the process is clearly present and nonrandom behavior exists. The error is due to a relative small number of truck groups (i.e. 16). The Runs Test assumes the distribution of the number of runs (R) is approximately normal when the number of truck groups (T) is large. Further, it is recommend the number of sampled truck groups should be larger than 20 (Stamatis, 2003). As a result, in the future the Runs Test will only be applied to a large sample of truck groups. Finally, the NA data did not indicate an out-of-control process. This is expected as the transverse stiffness alteration should not, theoretically, change the neutral axis position.

Removing the cross bracings connected to Girder 3 had an interesting effect on the lateral load distribution. The data shows the DF in Girder 4 increases while the DF in Girder 3 decreases. However, an increase in the Girder 3 DF is expected as removing the cross bracing should reduce the lateral load distribution to the surrounding girders. On-going bridge testing is being performed to further investigate this unusual behavior. Errors in constructing the bridge or the variable properties of timber may be an explanation for the observed behavior. Although the shift in DF cannot currently be explained, the SHM system was able to observe the unusual behavior, thus leading to further investigation.

3.8 Conclusion

This work has developed a SHM system to assess structural stiffness changes in timber bridges. The system uses strain measurements to report on the bridge condition. The developed data processing technique was demonstrated by installing a long-term Structural Health Monitoring (SHM) system on a demonstration timber bridge. The data processing technique was proven to perform the following functions:

- Detect and zero truck events.
- Determine approximate transverse truck position.
- Calculate stiffness parameters (i.e. distribution factors and neutral axis locations) from ambient traffic.
- Establish control limits on the stiffness parameters during a training period.
- Evaluate post-training data through statistical control chart techniques. The techniques include a set of control chart criterion and a Runs Test.
- Detect a change in transverse stiffness that was induced on the bridge by removing a set of cross bracings.

The continuous monitoring approach developed herein will provide owners with information regarding the structural integrity of their bridge in real time. As a result, maintenance decisions can be made earlier and more effectively. Furthermore, introducing structural health monitoring technologies into the timber bridge industry should result in improved safety, longer service life, and improved load ratings of timber bridges.

3.9 References

Bhattacharya, B., D. Li, M. Chajes, J. Hastings. "Reliability-Based Load and Resistance Factor Rating Using In-Service Data". Journal of Bridge Engineering, Vol, 10, No. 5, September 1, 2005.

Dyken, T.; Kepp, H. Monitoring the Moisture Content of Timber Bridges. Proceedings, International Conference Timber Bridges (ICTB), 2010. Lillehammer, Norway

Lu, P., "A Statistical Based Damage Detection Approach for SHM of Highway Bridges", Ph.D dissertation, Iowa State University, 2008.

Moore, J.C., R Glencross-Grant, Robert Patterson, "A review of Non-Destructive Test Methods: Appropriate Choice of a Method for use with Timber Beam Bridge Girders". World Conference on Tiber Engineering, 2010.

Phares, B., T. Hosteng, T. Pence, "The Development of a Smart Timber Bridge Utilizing Strain and Moisture Sensors". Report to the Forest Products Laboratory (FPL), Bridge Engineering Center, Iowa State University, 2013.

Stamatis, D. H. "Chapter 11: Control Chart Signals." Six Sigma and Beyond: Statistical Process Control. Boca Raton, FL: St. Lucie, 2003. 221-22. Print.

Vardeman, Stephen B., J. Marcus. Jobe, and Stephen B. Vardeman. Basic Engineering Data Collection and Analysis. Pacific Grove, CA: Brooks/Cole, 2001. Print.

CHAPTER 4 GENERAL CONCLUSIONS

This chapter provides an overview of the conclusions drawn from the journal papers presented in Chapters 2 and 3 and discusses how the conclusions benefit the timber bridge industry.

4.1 Strain and Moisture Sensor Evaluation

Chapter 2 focuses on timber specific sensing capabilities to evaluate deterioration and structural performance parameters. The general conclusions from Chapter 2 are:

- The relative humidity/temperature sensor was able to read moisture contents near 20% MC. However, the sensor was unable to be wired into an off-the-shelf data logger, making the sensor unappealing in structural health monitoring applications.
- The EMS was able to be wired into a data logging system; however, the sensor performed poorly with regard to moisture content accuracy. The sensor underestimated the moisture content by as much as 8%; therefore, the sensor was not selected for further evaluation.
- The optimal moisture sensor was the PMM sensor due to its reasonable accuracy, survivability under repeated loading, and ability to be wired into a complete data logging system. Thus, the sensor will be integrated into the smart system by strategically placing the sensor in areas of the bridge superstructure prone to water intrusion and early decay.
- Two methods (i.e. Shim and Patch) for embedding foil strain gages into glulam timber were successfully integrated into the glulam fabrication process. As a result, smart timber bridge component can be constructed without damaging the sensors.
- The Shim and Patch gages measured similar and consistent strains during fatigue and overload tests, thus providing reliability under repeated and extreme loadings. The reliability of the gages over the long-term makes them an appealing option for the smart timber bridge.

4.2 Data Processing Technique to Determine Changes in Structural Stiffness

Chapter 3 discusses a data processing technique that was developed to determine changes in timber bridge stiffness. The developed data processing technique was demonstrated by installing a long-term Structural Health Monitoring (SHM) system on a demonstration timber bridge. The data processing technique was proven to perform the following functions:

- Detect and zero truck events.
- Determine approximate transverse truck position.
- Calculate stiffness parameters (i.e. distribution factors and neutral axis locations) from ambient traffic.
- Establish control limits on the stiffness parameters during a training period.
- Evaluate post-training data through statistical control chart techniques. The techniques include a set of control chart criterion and a Runs Test.
- Detect a change in transverse stiffness that was induced on the bridge by removing a set of cross bracings.

4.3 Summary of Conclusions

From this work, the following contributions were added to the development of the smart timber bridge.

- A commercially available timber moisture sensor was selected for the smart timber bridge due its reasonable accuracy, survivability under repeated loading, and ability to be wired in to a complete data logging system.
- Two methods for embedding and attaching strain sensors into glulam girders were developed, tested, and successfully integrated into the glulam fabrication process.
- A data processing technique to evaluate structural stiffness parameters was successfully developed and implemented on an existing timber bridge.

The timber specific sensors and data processing techniques described herein collectively advance the development of a smart timber bridge. Upon completing the ongoing research plan, timber bridge owners will be provided with useful information regarding the performance and condition of their structure. As a result, owners will be able to program routine maintenance and/or rehabilitation in a more timely fashion. Furthermore, introducing

structural health monitoring technologies into the timber bridge industry should result in improved safety, longer service life, and improved load ratings of timber bridges.

4.4 Recommendations for Further Enhancements

4.4.1 Correcting Strain Magnitudes with Moisture Contents

The data processing technique described in Chapter 3 could be improved by considering seasonal moisture content variations. The modulus of elasticity (E) of timber is affected by changes in moisture content below the fiber saturation point. In general, the E increases with a decrease in moisture content. The variation in E due to seasonal changes may have a significant effect on the measured strain magnitudes; therefore, the strains should be corrected to eliminate fluctuations in moisture content. To do this, the E is calculated based on the measured moisture content using Equation 8 (Wood Handbook, 1999). Then, the strain is corrected to 12% moisture content using Equation 9.

$$E = E_{12}\left(\frac{E_{12}}{E_g}\right)^{\frac{12-M}{M_p-12}} \tag{8}$$

$$\varepsilon_{12} = \frac{E_{12}}{E}\varepsilon \tag{9}$$

Where:

E = modulus of elasticity at moisture content M (%)

E_{12} = modulus of elasticity at 12% moisture content (tabulated value)

E_g= modulus of elasticity for green wood

M_p = 25 for Southern Yellow Pine

ε = measured strain

ε_{12} = corrected strain to 12% moisture content

Correcting strain values to 12% moisture content provides a level of consistency and should eliminate some variability in the process. Specifically, correcting strains may lead to

less false positive alarms that might occur in seasons in which the training period was not conducted.

4.4.2 Optimal Truck Group Size and Control Criteria Leading to Further Investigation

The selection of group size directly affects the control limits and thus affects the sensitivity of control charts. The truck group size of 5 used in the change in stiffness algorithm was selected based on judgment and no analysis was performed to determine an optimal truck group size. Therefore, an optimal truck group size should be determined for this particular system. Consideration should be given to both large and small truck group sizes. The advantage of large truck group sizes is narrower control limits, thus allowing small variations in the process to be detected. However, if the truck group is too large, a detection delay occurs since the system is not alarmed until an entire truck group passes over the bridge. A study should be conducted to select a truck group size that achieves an appropriate balance between the advantages and disadvantages of small and large group sizes.

In addition to truck group size, a study should be conducted to determine the appropriate time to respond to out-of-control signals indicated by the control chart criterion. As mentioned in Chapter 3, out-of-control signals occasionally exist when no change in the bridge behavior is present. Responding to each false-positive event can be time consuming and expensive. The study should investigate the occurrence of false-positive alarms during damaged and undamaged conditions. The results from the study should provide specific control chart criteria and number of occurrences that required an engineer to take action.

4.4.3 Implementing the Change in Stiffness Algorithm into other Bridges

The developed change in stiffness algorithm presented in Chapter 3 can be easily implemented into other bridge types. In fact, the system would be more successful in bridges with well-defined traffic lanes. For example, consider a two lane bridge with a superstructure consisting of multiple steel girders and a concrete deck. In this case, two distribution factor control charts can be constructed that correspond to each of the traffic lanes. Deck-bottom strain gages would be used to determine if the vehicle is travelling in Lane 1 or Lane 2. The distribution factor data for a truck traveling in Lane 1, for instance, would be compared

against the control limits set for Lane 1 events.

Using two control charts for each lane has a couple advantages. First, more primarily loaded girders are evaluated, thus allowing changes in stiffness to be determined more effectively. Furthermore, exterior girders experience greater loads in the two-lane system as compared to center events. This allows exterior girders to be evaluated for changes in stiffness. Finally, the data are used more efficiently when two lanes are considered. In the current system, several data files were not used because the center event criteria were not satisfied. Increasing the amount of useful data would likely result in a more efficient system.

Monitoring the neutral axis location in a typical steel-girder bridge can also provide an indication of a stiffness change. If the neutral axis is above the steel-concrete interface then a portion of the deck is in tension, potential leading to cracking. The neutral axis also gives an indication of composite action. The neutral axis location is expected to move downward as the deck deteriorates and loses composite action. In general, any questionable movement of the neutral axis location over time should be further investigated.

4.4.4 Additional Recommendations

- Calibration of the PMM sensor could be conducted to achieve more accurate results, particularly near 20% moisture content. The system calibration may entail altering the equations relating moisture content, electrical resistance, wood species, and temperature to match moisture content measurements obtain from gravimetric results and/or a moisture meter. Additionally, altering the wiring schematic may aid in the calibration. Experimenting with different excitation voltages and reference resistors may provide greater accuracy around 20% MC.
- Building on the developed system, the research team should develop techniques for identifying vehicle impacts to the guard rail.
- The data processing technique should be automated to reduce the amount of "manual" data reduction. This may be done in the software development phase of the research plan.

4.4.5 Future Smart Timber Research

The next phase in the Smart Timber Bridge Research Plan is to develop a data processing technique for determining truck loading characteristics. By determining vehicle characteristics, it will be possible to better predict usage and induced damaged. After this phase is completed, the next phase is to develop a software application for the smart timber bridge. The software is envisioned to collect, extract, analyze, and report on the health condition of the structure. The final task of the research plan is to demonstrate all the developed components by constructing an actual smart timber bridge. This entails preparing detailed construction plans and specifications for the assembly of the smart timber bridge components. This comprehensive effort will result in the first fully automated structural health monitoring system for timber bridges.